


Article

Molecular and Carbon Isotopic Compositions of Crude Oils from the Kekeya Area of the Southwest Depression, Tarim Basin: Implications for Oil Groups and Effective Sources

Xiaojie Gao ¹, Qilin Xiao ^{1,*}, Zhushi Ge ¹, Suyang Cai ¹, Haizhu Zhang ², Xiang Wang ², Zhenping Xu ², Zhanghu Wang ¹, Xiaomin Xie ¹  and Qiang Meng ¹

¹ Key Laboratory of Oil and Gas Resources and Exploration Technology, College of Resources and Environment, Yangtze University, Wuhan 430100, China; xiaojiegao.stu@yangtzeu.edu.cn (X.G.)

² Research Institute of Exploration and Development, PetroChina Tarim Oilfield Branch, Korla 841000, China

* Correspondence: qilinxiao@cug.edu.cn

Abstract: Molecular and stable carbon isotopic compositions of 32 crude oils from the Kekeya area of the Southwest Depression, Tarim Basin, were analyzed comprehensively to clarify oil groups and trace oil sources. The results indicate that lacustrine shale sequences within the Upper-Middle Permian Pusige Formation (P_{3-2p}) are the major effective oil sources; the thermal maturation effects exert the crucial impact on geochemical compositions of crude oils. In the Kekeya structural belt, crude oils produced from the Lower-Neogene, Middle-Paleogene and Middle-Cretaceous sandstone reservoirs were generated mainly from deeply buried P_{3-2p} at the late-to-high maturity stage. These condensates are depleted in terpanes, steranes and triaromatic steranes and enriched in adamantanes and diamantanes. The evaluated thermal maturity levels of crude oils by terpanoids and steranes are generally lower than that of diamondoids, implying at least two phases of oil charging. In the Fusha structural belt, oils produced from the Lower-Jurassic reservoirs (J_{1s}) of Well FS8 were generated from the local P_{3-2p} at the middle to late mature stage. On the contrary, these oils are relatively rich in molecular biomarkers such as terpanes and steranes and depleted in diamondoids with only adamantanes detectable. The P_{3-2p}-associated oils can migrate laterally from the Kekeya to Fusha structural belt, but not to the location of Well FS8. The Middle-Lower Jurassic (J₁₋₂) lacustrine shales as the major oil sources are limited to the area around Well KS101 in the Kekeya structural belt. Crude oils originated from J₁₋₂ and P_{3-2p} can mix together within the Cretaceous reservoirs of Well KS101 by presenting the concurrence of high concentrations of terpane and sterane biomarkers and diamondoids as well as 2–4% ¹³C-enriched *n*-alkanes than those of P_{3-2p} derived oils. This study provides a better understanding of hydrocarbon sources and accumulation mechanisms and hence petroleum exploration in this region.

Keywords: Tarim Basin; Kekeya area; biomarkers; diamondoids; carbon isotope; oil sources



Citation: Gao, X.; Xiao, Q.; Ge, Z.; Cai, S.; Zhang, H.; Wang, X.; Xu, Z.; Wang, Z.; Xie, X.; Meng, Q. Molecular and Carbon Isotopic Compositions of Crude Oils from the Kekeya Area of the Southwest Depression, Tarim Basin: Implications for Oil Groups and Effective Sources. *Energies* **2024**, *17*, 760. <https://doi.org/10.3390/en17030760>

Academic Editor: Hossein Hamidi

Received: 7 January 2024

Revised: 30 January 2024

Accepted: 1 February 2024

Published: 5 February 2024



Copyright: © 2024 by the authors. Licensee MDPI, Basel, Switzerland. This article is an open access article distributed under the terms and conditions of the Creative Commons Attribution (CC BY) license (<https://creativecommons.org/licenses/by/4.0/>).

1. Introduction

The Southwestern Depression of Tarim Basin is a typical foreland basin developed in Miocene and Pliocene [1] (Figure 1a). The Kekeya Oilfield is located at the southwestern margin of the Southwest Depression [1] (Figure 1b), which was formed during the Pliocene to Early Pleistocene [2]. The current oil reserves of around 19.0 million tones have been proved to be hosted in the Lower-Neogene, Middle-Paleogene and Cretaceous sandstone reservoirs [2] (Figure 2). This suggests the promising potential for hydrocarbon exploration and exploitation in this region [3]. The discovery of the Kekeya Oilfield is hence considered to be the second important milestone for petroleum exploration in the Tarim Basin [4].

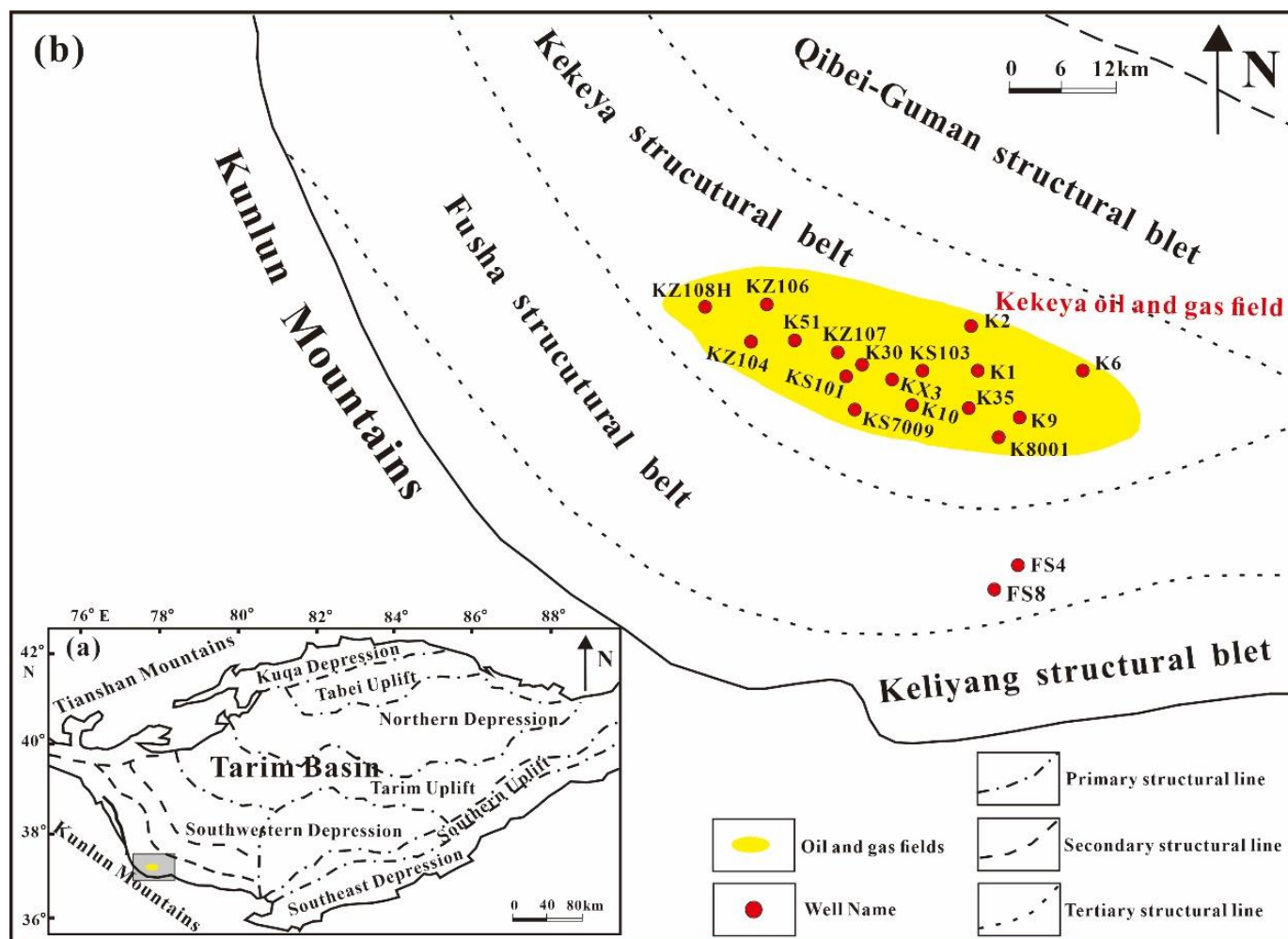


Figure 1. (a) The location of study area and (b) the tectonic elements and well distribution of the Kekeya area (modified after [5]).

Two sets of hydrocarbon source rocks have been disclosed in the Kekeya area. They are composed of the Permian lacustrine mudstones within the Pusige Formation and the Middle-Lower Jurassic sequences [3]. Specifically, the Permian lacustrine mudstones in the Pusige Formation contain mainly Type II kerogen with the TOC value of 0.33–4.19% and have entered into the high mature stage with $\%Ro = 0.84\text{--}1.40$ [6,7]. The extractable biomarkers within source rocks are enriched in the unknown C_{30} terpenoids, C_{29} and C_{30} rearranged hopanes and C_{29} regular steranes [8,9]. The $\delta^{13}C$ values of individual n -alkanes range from -34.0% to -28.0% , indicating the major role of aquatic organic matter inputs within the Permian Pusige shale sequences. [9,10].

The Jurassic source rocks were deposited in the fluvial/lacustrine bog setting and contain mainly Type II kerogen within the shales and Type III kerogen within the coaly shales and coals [3,6]. The Middle-Lower Jurassic source rocks are depleted in C_{30} rearranged hopanes and C_{27} -trisnorhopane (Ts) and also enriched in C_{29} regular steranes with the $C_{29} \alpha\alpha\alpha 20S/(20S + 20R)$ value of <0.3 , indicating the immature and/or low-matured organic matters within the Jurassic source rocks [6,11,12]. The $\delta^{13}C$ values of Jurassic kerogens range from -27.2% to -23.3% [3,13].

The occurrence of multiple source rocks results in a big challenge of hydrocarbon sources in this region. In general, four opinions have been proposed:

- (I). Jurassic source rocks. At the early stage of petroleum exploration, the Carboniferous, Permian and Jurassic source rocks were discovered in the northern area of the southwestern margin of the Tarim Basin, the Carboniferous and Permian source rocks were

deposited in the marine setting and the Jurassic source rocks were deposited in the terrestrial environments [3,14]. Previous investigators thought that these three sources were also developed in the Kekeya area. The occurrence of spore pollen, $V/Ni < 1$ and the enrichment of C_{29} regular steranes for crude oils from the Kekeya Oilfield led some investigators to believe that crude oils were generated mainly from the Jurassic lacustrine source rocks [15], since the spore pollen can only be detected in the Jurassic Yangye Formation [3,15];

- (II). Permian shales. Some investigators have suggested that crude oils from the Kekeya Oilfield were originated mainly from the Permian source rocks, the relevant evidence refers to the enrichments of Ts, C_{30} rearranged hopanes, and C_{27} or C_{29} regular steranes and depletion of hopanes in oils. The $\delta^{13}C$ value of individual *n*-alkanes range from -32% to -28% [6,8–10];
- (III). Permian and Jurassic source rocks. Diterpenoids are considered to be the typical biomarkers to indicate the inputs of higher plants [16]. With the development of petroleum exploration in this region, these compounds were detected in the newly produced crude oils, and these oils are isotopically 2–3% heavier than the Permian-sourced oils. The higher plants act as the major role in the Jurassic source rocks [5]. This indicates that except for the Permian lacustrine shales, the Jurassic source rocks may also have a major contribution [5];
- (IV). Carboniferous and Permian source rocks. Crude oils from the Kekeya Oilfield are relatively enriched in dibenzothiophene, tricyclic and tetracyclic diterpanes and 3β -methyl steranes [17,18]. This indicates that these oils may be originated from pre-Mesozoic formations. The $\delta^{13}C$ values of saturated and aromatic fractions suggest the mixed contributions of terrigenous and aquatic alge [19]. These two lines of evidence highlight the major contribution of Carboniferous and Permian source rocks in study area [19]. In fact, only the Permian lacustrine shales and Jurassic source rocks were discovered in this region later [8,11].

The abovementioned research arrives at the relevant conclusions regarding oil sources based mainly on the geochemical data of small pieces of oil samples in the Kekeya structural belt, hence introducing the unpredictable uncertainty into the whole map of oil sources in this region. More recently, a new discovery well, Well FS8, was drilled in the Fusha structural belt (Figure 1b). Crude oils were produced from the Lower-Jurassic Shalitashi sandstone reservoirs with the daily production of 20.6 m^3 (Figure 2) [20]. This highlights the promising potential of hydrocarbon resources in the Fusha structural belt. However, several questions induced by this new discovery: where is this oil derived mainly from? Is it generated from the local source rocks or a migrated oil from the Kekeya structural belt? Is this oil similar to oils from the neighbor Well FS4 in the Fusha structural belt? All these questions require us to make a comprehensive reevaluation of hydrocarbon sources in this region. Accordingly, 32 oil samples were collected from the Fusha and Kekeya structural belts; this study focuses on the molecular and stable carbon isotopic compositions of these oil samples to clarify the whole map of oil groups and their possible hydrocarbon sources. The result provides a better understanding of hydrocarbon sources and accumulation mechanisms and hence petroleum exploration in this region.

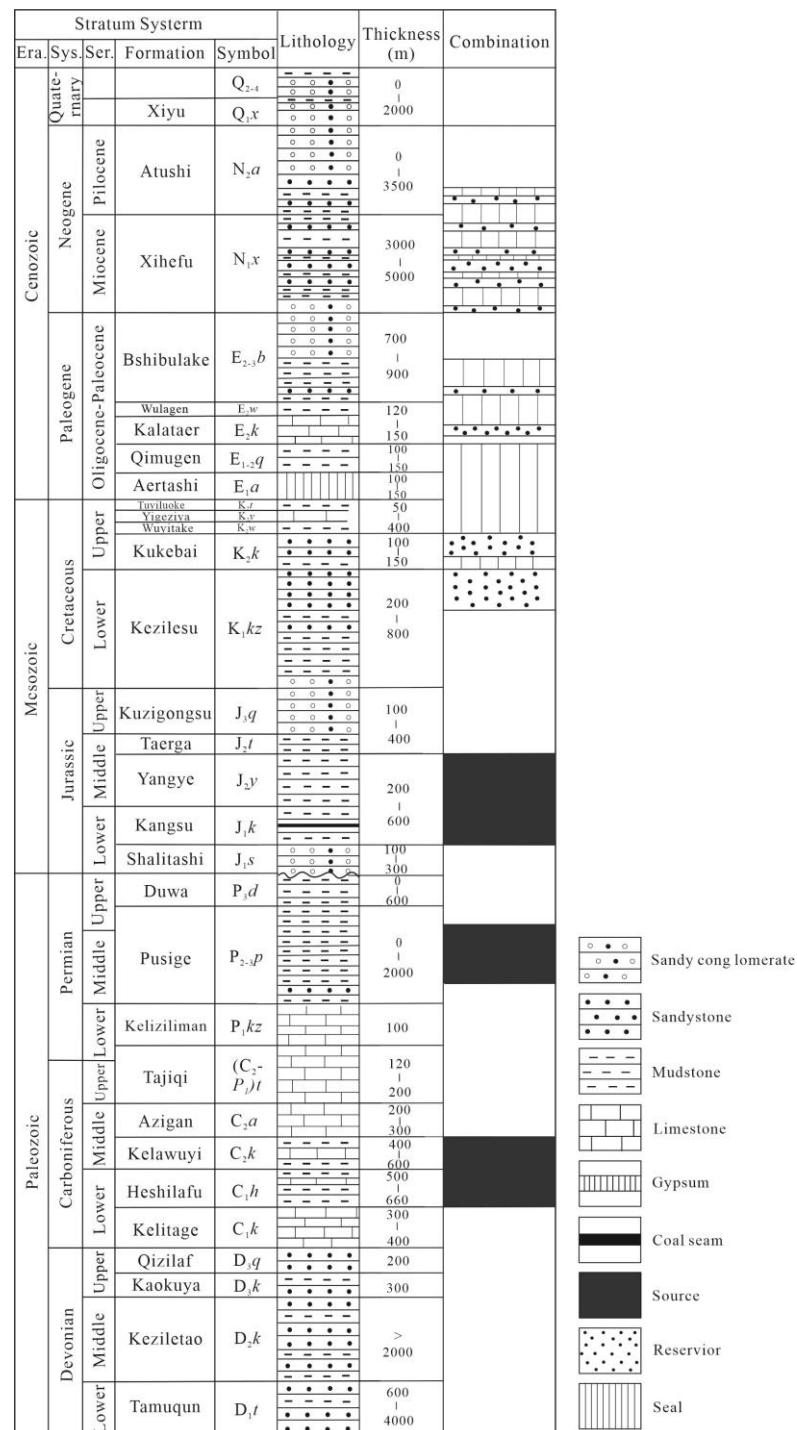


Figure 2. Comprehensive stratigraphy histogram of the Southwest Depression, Tarim Basin (modified after [21]).

2. Samples and Methods

2.1. Oil Samples

A total of 32 oil samples were collected from the Kekeya area (Figure 1 and Table 1), including 20 samples from the Lower Neogene Xiehefu Formation (N_{1x}), 5 samples from the Middle Paleogene Kalataer Formation (E_{2k}), 3 samples from the Middle Cretaceous Kukebai Formation (K_{2k}), 2 samples from the Middle Cretaceous Kezilesu Formation (K_{1kz}) and 2 oil samples from the Lower-Jurassic Shalitashi reservoir (J_{1s}) (Figure 1). Most oils are the condensate, while 2 J_{1s} samples are the normal oil.

Table 1. Molecular parameters and concentrations of terpanes and steranes for oil samples from the Kekeya area.

Oil Group	Well	Depth (m)	Formation	C ₁₉ -C ₂₃ TT/ C ₃₀ H	C ₂₄ Ter/ C ₂₆ TT	Ts/ (Ts + Tm)	DiaC ₃₀ H/ C ₃₀ H	Ga/ C ₃₀ H	C ₂₉ - $\alpha\alpha\alpha$ 20S/ (20S + 20R)	C ₂₉ - $\alpha\beta\beta$ / ($\alpha\beta\beta$ + $\alpha\alpha\alpha$)	C ₁₉₋₂₃ TT ($\mu\text{g/g}$)	DiaC ₃₀ H ($\mu\text{g/g}$)	C ₃₀₋₃₅ H ($\mu\text{g/g}$)	Regular Sterane ($\mu\text{g/g}$)		
														C ₂₇	C ₂₈	C ₂₉
Group I	KS101	6664	K ₁	0.6	1.5	0.4	0.1	0.2	0.4	0.4	268	48	1548	40	84	289
		6821	K ₁	0.7	1.2	0.4	0.1	0.2	0.4	0.4	500	43	2647	69	132	452
Group II	FS8	3882	J _{1s}	0.3	3.0	0.5	0.2	0.0	0.5	0.5	302	180	2620	26	226	614
		3899	J _{1s}	0.3	3.0	0.5	0.2	0.0	0.5	0.5	285	177	2500	28	222	599
Group III	FS4	2394	K ₂	1.1	2.0	0.7	0.6	0.1	0.6	0.6	252	147	649	13	78	214
	FS4	2396	K ₂	1.2	2.0	0.7	0.6	0.1	0.5	0.5	178	96	411	11	50	140
	FS4	2789	K ₂	1.4	1.4	0.8	0.7	0.1	0.5	0.6	139	75	283	9	33	99
	KS103	6336	E _{2k}	4.2	1.1	0.8	1.8	0.1	0.5	0.6	196	91	136	11	58	147
	KZ108H	6755	E _{2k}	3.2	1.2	0.8	1.1	0.1	0.5	0.6	216	77	182	10	50	129
	K2	3323	N ₁	3.8	1.3	0.8	1.6	0.3	0.5	0.5	167	76	142	17	69	172
	K2	3776	N ₁ x ₇ ²	3.6	0.7	0.6	0.3	0.2	0.5	0.5	2	0	1	0	1	2
	K10	/	N ₁	1.0	0.5	0.7	0.5	0.3	0.5	0.5	13	8	39	1	14	33
	KS7009	3877	N ₁ x ₇ ²	0.7	0.8	0.7	0.4	0.4	0.5	0.5	123	72	440	22	57	154
KS7009	3944	N ₁ x ₇ ²	3.4	0.9	0.8	1.7	0.3	0.5	0.5	153	82	132	13	52	131	
Group IV	K1	/	N ₁	12.9	1.4	0.9	3.8	0.4	0.5	0.5	99	32	26	8	23	55
	K2	3172	N ₁ x ₄ ¹	12.5	0.8	0.8	1.3	0.0	0.4	0.5	15	2	2	0	1	2
	K2	3221	N ₁ x ₄ ²	8.8	1.1	0.7	1.9	0.1	0.6	0.5	10	2	1	0	2	5
	K2	3273	N ₁	7.5	1.3	0.8	3.3	0.4	0.5	0.6	119	57	42	6	22	52
	K2	3804	N ₁ x ₈	6.6	1.0	0.6	0.5	0.2	0.4	0.4	58	4	16	10	9	26
	K6	3322	N ₁ x ₄	7.1	0.9	0.7	2.8	0.4	0.5	0.6	55	24	21	11	56	145
	K9	3030	N ₂	6.1	1.5	0.8	1.5	0.2	0.5	0.5	88	22	38	9	21	54
	K9	3101	N ₁	11.1	1.0	0.7	2.9	0.1	0.5	0.6	5	1	0	0	1	2
	K9	3871	N ₁	6.1	0.9	0.7	5.0	0.2	0.5	0.5	71	17	26	10	19	50
	K30	3805	N ₁ x ₅	11.9	0.8	0.9	2.9	0.3	0.5	0.6	16	4	5	1	3	6
	K35	/	N ₁ x ₅ ²	30.5	1.0	0.6	2.9	0.3	0.3	0.6	7	0	0	0	0	1
	K51	3703	N ₁ x ₂	27.5	0.9	0.7	3.9	0.7	0.5	0.6	13	2	2	0	1	3
	K8001	3929	N ₁ x ₈	10.3	0.7	0.7	1.9	0.3	0.5	0.6	11	2	3	0	2	3
	KX3	3793	N ₁ x ₈	11.0	1.0	0.8	1.2	0.3	0.5	0.5	69	9	21	3	3	9
	KS103	3867	N ₁ x ₈	15.9	1.1	0.9	3.4	0.4	0.5	0.5	104	24	21	8	18	48
	KZ104	6348	E	8.1	0.9	0.9	3.5	0.4	0.5	0.6	103	47	40	11	31	80
	KZ106	/	E _{2k}	8.7	0.9	0.9	3.7	0.3	0.5	0.6	109	48	49	9	28	76
KZ107	6269	E	9.1	1.1	0.8	2.7	0.2	0.5	0.6	92	30	40	8	19	49	

Note: C₁₉-C₂₃TT: the total concentrations of C₁₉-C₂₃ tricyclic terpanes; C₃₀H: C₃₀17 α (H), 21 α (H)-hopane; C₂₄Ter: C₂₄ tetracyclic terpene; C₂₆TT: C₂₆ tricyclic terpanes; Ts: C₂₇18 α (H), 21 β (H)-22, 29, 30-trisnorhopane; Tm: C₂₇17 α (H), 21 β (H)-22,29,30-trisnorhopane; DiaC₃₀H: C₃₀17 α (H)-diahopane; Ga: Gammacerane; C₃₀₋₃₅H: the total concentrations of C₃₀-C₃₅ hopanes.

2.2. Gas Chromatography (GC)

The whole oil GC traces were obtained by using the Agilent 7890B gas chromatograph equipped with a flame ionization detector (FID). A fused silica capillary column (50 m × 0.32 mm i.d.) coated with CP-SIL5CB (film thickness 0.40 mm) was used. The sample was injected using a split ratio of 50:1 and nitrogen was used as carrier gas, with a constant flow rate of 1.0 mL/min. The GC oven was initially set at 35 °C for 15 min, subsequently programmed to 310 °C at 4 °C/min and then maintained at this temperature for 30 min [22]. Although the whole oil GC traces can be used to calculate the parameters including $\sum n\text{-C}_{21-}/\sum n\text{-C}_{22+}$, carbon preference index (CPI) and odd-even predominance (OEP) of *n*-alkanes, Pr/Ph, Pr/*n*-C₁₇ and Ph/*n*-C₁₈ (Table 2), the quantification of specific compounds needs to run these samples on the gas chromatography-mass spectrometry (GC-MS).

Table 2. Molecular parameters and concentrations of *n*-alkanes and isoprenoids for oil samples from the Kekeya area.

Oil Group	Well	Depth (m)	Formation	Main Peak	$\sum n\text{-C}_{21-}/\sum n\text{-C}_{22+}$	CPI	OEP	Pr/Ph	Pr/ <i>n</i> -C ₁₇	Ph/ <i>n</i> -C ₁₈	<i>n</i> -Alkanes (μg/g)	
Group I	KS101	6664	K ₁	<i>n</i> -C ₁₄	4.02	1.08	0.89	1.25	0.06	0.05	358,636	
		6821	K ₁	<i>n</i> -C ₁₄	3.10	1.14	0.90	1.08	0.08	0.09	314,590	
Group II	FS8	3882	J _{1s}	<i>n</i> -C ₂₁	3.05	1.04	0.95	1.53	0.15	0.10	254,729	
		3899	J _{1s}	<i>n</i> -C ₂₁	3.01	1.11	0.94	1.55	0.16	0.10	264,203	
Group III	KS103	FS4	2394	K ₂	<i>n</i> -C ₁₃	3.34	1.19	0.91	1.65	0.08	0.06	303,792
		FS4	2396	K ₂	<i>n</i> -C ₁₃	4.83	1.19	0.92	1.78	0.08	0.05	417,742
		FS4	2789	K ₂	<i>n</i> -C ₁₃	2.96	1.11	0.93	1.54	0.06	0.04	612,909
		KS103	6336	E _{2k}	<i>n</i> -C ₁₂	3.48	1.09	0.92	1.16	0.08	0.07	307,870
		KZ108H	6755	E _{2k2}	<i>n</i> -C ₈	3.05	1.09	0.93	1.18	0.07	0.06	335,809
		K2	3323	N ₁	<i>n</i> -C ₁₁	2.85	1.13	0.95	1.55	0.16	0.10	218,293
		K2	3776	N _{1x7} ²	<i>n</i> -C ₁₀	23.49	1.13	0.93	1.23	0.07	0.06	495,750
		K10	/	N ₁	<i>n</i> -C ₁₂	20.47	1.08	0.94	1.38	0.07	0.06	475,483
		KS7009	3877	N _{1x7} ²	<i>n</i> -C ₁₃	2.78	1.09	0.92	1.06	0.06	0.06	325,145
		KS7009	3944	N _{1x7} ²	<i>n</i> -C ₁₀	3.50	1.10	0.93	1.02	0.06	0.06	436,337
Group IV	KS103	K1	/	N ₁	<i>n</i> -C ₁₅	3.80	1.10	0.9	1.27	0.07	0.06	482,465
		K2	3172	N _{1x4} ¹	<i>n</i> -C ₁₀	19.57	1.14	0.64	1.23	0.07	0.07	466,475
		K2	3221	N _{1x4} ²	<i>n</i> -C ₉	10.45	1.10	0.92	1.2	0.07	0.06	425,773
		K2	3273	N ₁	<i>n</i> -C ₁₄	2.81	1.09	0.96	1.1	0.07	0.06	295,270
		K2	3804	N _{1x8}	<i>n</i> -C ₁₀	26.11	1.16	0.92	1.38	0.07	0.06	474,613
		K6	3322	N _{1x4}	<i>n</i> -C ₁₅	2.67	1.11	0.92	1.12	0.06	0.06	418,273
		K9	3030	N ₂	<i>n</i> -C ₁₂	6.46	1.12	0.93	1.18	0.06	0.06	258,799
		K9	3101	N ₁	<i>n</i> -C ₁₃	4.21	1.15	0.93	1.67	0.09	0.06	239,626
		K9	3871	N ₁	<i>n</i> -C ₁₂	6.57	1.10	0.94	1.19	0.06	0.06	389,962
		K30	3805	N _{1x5}	<i>n</i> -C ₁₁	7.30	1.11	0.94	1.12	0.06	0.05	483,963
		K35	/	N _{1x5} ²	<i>n</i> -C ₁₁	32.40	1.04	0.95	1.22	0.10	0.07	358,932
		K51	3703	N _{1x2}	<i>n</i> -C ₁₂	7.60	1.12	0.92	1.21	0.07	0.06	438,024
		K8001	3929	N _{1x8}	<i>n</i> -C ₁₀	8.61	1.10	0.95	1.16	0.06	0.06	506,190
		KX3	3793	N _{1x8}	<i>n</i> -C ₁₀	20.18	1.10	0.62	1.84	0.10	0.07	482,712
		KS103	3867	N _{1x8}	<i>n</i> -C ₁₁	6.68	1.10	0.92	1.10	0.07	0.07	499,034
		KZ104	6348	E	<i>n</i> -C ₉	5.39	1.11	0.93	1.17	0.06	0.05	354,246
		KZ106	/	E _{2k}	<i>n</i> -C ₁₀	4.89	1.11	0.92	1.13	0.06	0.05	284,251
KZ107	6269	E	<i>n</i> -C ₉	5.70	1.10	0.90	1.21	0.06	0.05	342,163		

Note: CPI = $\{(C_{25} + C_{27} + C_{29} + C_{31} + C_{33}) [1/(C_{24} + C_{26} + C_{28} + C_{30} + C_{32}) + 1/(C_{26} + C_{28} + C_{30} + C_{32} + C_{34})]\} / 2$; OEP = $\{(C_i + 6 \times C_{i+2} + C_{i+4}) / [4 \times C_i + 1 + C_{i+3}]\} m, i + 2$; Main peak carbon, m: $(-1) i + 1$.

2.3. Gas Chromatography-Mass Spectrometry (GC-MS)

Asphaltenes were removed by precipitation with *n*-hexane followed by filtration. The de-asphalted oils were then separated into saturated, aromatic and resins fractions using column chromatography with aluminum oxide as stationary phase, with *n*-hexane, benzene, and a mixture of dichloromethane and methanol (9:1, *v/v*) as eluents, respectively. The measurements of GC-MS were conducted on the saturated and aromatic fractions. Prior to GC-MS analysis, two internal standards squalane and adamantane-d₁₆ were added for the quantification of terpenes, steranes, diamondoids and aromatic compounds, respectively.

The GC-MS was equipped with a Hewlett-Packard 6890 gas chromatograph coupled to a Micromass Platform II spectrometer. The HP-5MS column (30 m \times 0.25 mm i.d. \times 0.25 μ m) was used for the separation. The GC oven temperature was initially held at 60 °C for 2 min, ramped from 60 °C to 315 °C at 3 °C/min and held for 15 min. The carrier gas was helium, and the flow rate was 1.0 mL/min. The temperature was 250 °C for transfer line and 200 °C for the ion source. The operation conditions of ion source were the electron ionization (EI) mode at 70 eV. The identification of targeted compounds was performed by the Full scan and SIM GC-MS analysis. The mass range was 50–550 Da with the scan time of 1 s for full scan GC-MS analysis [23]. The selected ions of SIM GC-MS analysis were m/z 85 for *n*-alkanes, m/z 135, 136, 149, 163 and 177 for adamantanes, m/z 187, 188, 201 and 215 for diamantanes, m/z 191 for terpanoids, m/z 217 for steranes, m/z 178 and 192 for phenantheranes, m/z 184 and 198 dibenzothiophenes (DBTs), m/z 231 for triaromatic steroids and m/z 85 for squalane and m/z 152 for adamantane- d_{15} [23]. Although the quantitative data can be obtained by using GC-MS analysis, gas chromatography isotope ratio mass spectrometry (GC-IRMS) is required to get the stable carbon isotopic compositions of individual *n*-alkanes.

2.4. Gas Chromatography Isotope Ratio Mass Spectrometry (GC-IRMS)

Stable carbon isotopic compositions of individual compounds were analyzed by a Hewlett-Packard 6890 gas chromatograph connected to a Micromass Isoprime system. HP6890 GC was fitted with a 50 m \times 0.32 mm i.d. column coated with a 0.40 μ m film of CP-SIL 5CB, leading directly into the combustion interface. The oven temperature was as follows: 30 °C for 15 min, raised from 30 °C to 310 °C at a rate of 3 °C/min and held at 310 °C for 30 min. Helium was used as the carrier gas with a flow rate of 1.5 mL/min. The sample was injected using a split mode with a split ratio of 15:1. The combustion furnace was operated at a temperature of 800 °C and was equipped with CuO and Pt wire as oxidant and catalyst. In order to perform calibration, a CO₂ reference gas calibrated against Charcoal Black (a national calibration standard, with a value of –22.43% based on the VPDB standard) was automatically introduced into the IRMS in a series of pulses before and after the array of peaks of interest [22]. The precision of the measurement was typically better than 0.3% relative to the VPDB standard.

3. Results

3.1. Terpenoids, Steranes and Oil Groups

Figure 3 and Table 1 present the chemical compositions of terpenoids and steranes for oil samples from the Kekeya area. Significant differences can be detected on steranes, in particular terpenoids. Based on the distribution patterns of terpenoids and steranes, oil samples from the Kekeya area are classified into four groups:

- (1) Group I: oil samples from KS101. These samples are depleted in tricyclic terpanes, Ts, C₃₀H rearranged hopane and enriched in C₂₉ Norhopane, C₃₀–C₃₅ hopanes and C₂₉ steranes (Figure 3a), resulting in low ratios of C₁₉–C₂₃TT/C₃₀H, Ts/(Ts + Tm) and DiaC₃₀H/C₃₀H (Table 1). C₂₀ TT is the peak of C₁₉–C₂₃TT (Figure 3a). Regular steranes decrease with the order of C₂₉ $\alpha\alpha\alpha$ 20R > C₂₇ $\alpha\alpha\alpha$ 20R > C₂₈ $\alpha\alpha\alpha$ 20R (Figure 3a);
- (2) Group II: oil samples from FS8. Compared with Group I oils, these oils contain more C₂₉ norhopane, C₃₀ rearranged hopane and C₂₉ steranes, resulting in higher ratios of DiaC₃₀H/C₂₉Ts and C₂₉ $\alpha\alpha\alpha$ 20R/C₂₇ $\alpha\alpha\alpha$ 20R, C₂₃ TT is the peak of C₁₉–C₂₃TT (Figure 3b and Table 1).
- (3) Group: oil samples from FS4, KZ104, KZ106, KZ107, KZ108H, K6, KS7009, K2 (N_{1x5}) and KS103 (E_{2k}). Compared with Group I/II oils, Group III oils contain much less C₁₉–C₂₃TT, C₃₀–C₃₅ hopanes and C₂₇–C₂₉ steranes, but present much higher ratios of C₁₉–C₂₃TT/C₃₀H, Ts/(Ts + Tm), DiaC₃₀H/C₃₀H (Figure 3c and Table 1).
- (4) Group IV: oil samples from K1, K2 (N_{1x4}, N_{1x7}, N_{1x8}), K9, K10, K30, K35, K51, K8001, KX3 and KS103 (N_{1x8}). These oils are even more depleted in C₁₉–C₂₃TT, C₃₀–C₃₅ hopanes and C₂₇–C₂₉ steranes than Group III oils (Figure 3d). The ratios of C₁₉–

$C_{23}TT/C_{30}H$, $DiaC_{30}H/C_{30}H$ and $C_{29} \alpha\alpha\alpha 20R/C_{27} \alpha\alpha\alpha 20R$ are greater than those for Group III oils (Table 1).

Except for terpenoids and steranes, the molecular compositions of these collected oil samples are comprehensively depicted quantitatively including *n*-alkanes, isoprenoids and diamondoids in the saturated fraction and naphthalenes, phenanthrenes, dibenzothiophenes and triaromatic steranes in the aromatic fraction. The results of compound-specific carbon isotope analysis of *n*-alkanes were also provided to make a more sophisticated geochemical map of these oil samples at the molecule levels. The details are stated as the following.

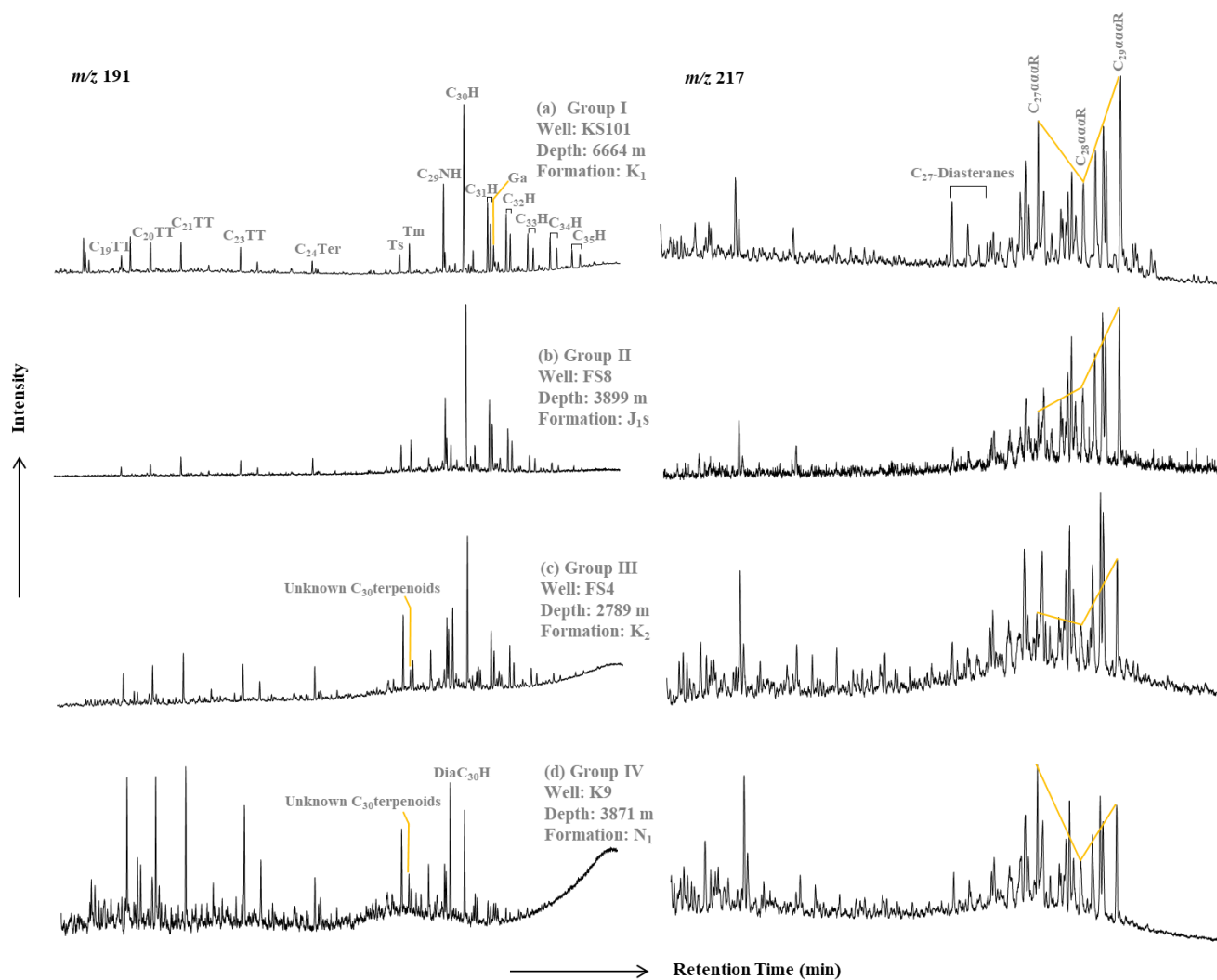


Figure 3. Typical m/z 191 and m/z 217 mass chromatograms showing the distribution of the terpanes and steranes in four oil groups from the Kekeya area.

3.2. *n*-Alkanes and Isoprenoids

Figure 4 presents the typical GC traces of whole oils. Group I oils have the main peak of *n*-C₁₄ and high concentrations of *n*-alkanes. Group II oils have the bimodal distribution of *n*-alkanes with the main peaks of *n*-C₁₁ and *n*-C₂₁. Group III/IV oils have the main peak ranging from *n*-C₈ to *n*-C₁₅ and also high concentrations of *n*-alkanes. Moreover, the $\Sigma n-C_{21-} / \Sigma n-C_{22+}$ ratio for Group III/IV oils is obviously greater than that for Group I/II oils. No significant difference can be observed on the other parameters (Table 2).

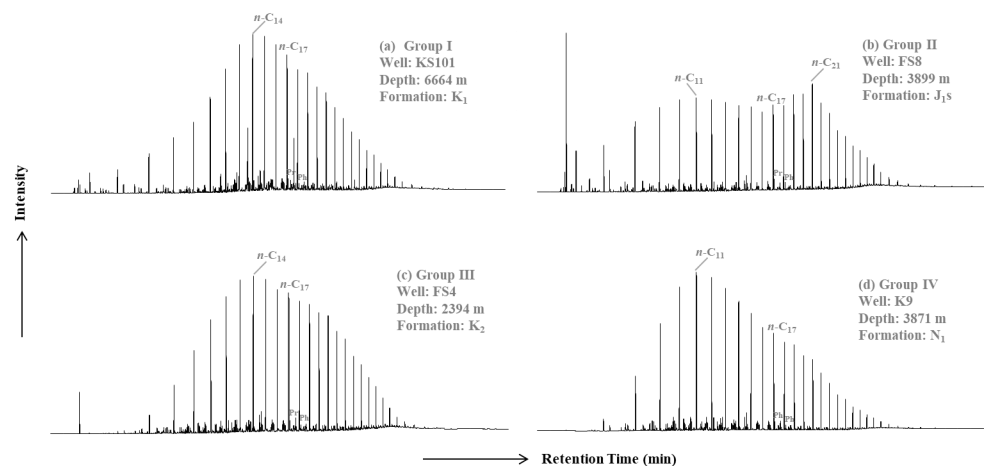


Figure 4. Typical GC traces of crude oils within four groups in the Kekeya area.

3.3. Diamondoids

Figure 5 and Table 3 present the molecular compositions of diamondoids in crude oils collected from the Kekeya area. 1-cage adamantanes and 2-cage diamantanes comprise the diamondoids for crude oil samples (Figure 5). Group I oils have the highest concentrations of diamondoids (35,763–45,244 $\mu\text{g/g}$) and the highest ratios of MAI and MDI (Table 3). In contrast, Group II oils have the lowest concentrations of diamondoids (147–148 $\mu\text{g/g}$) and contain only adamantanes with no diamantanes detectable (Table 3). The concentrations of diamondoids are 941–2001 $\mu\text{g/g}$ for Group III oils and 755–3884 $\mu\text{g/g}$ for Group IV oils, which are much lower than group I oils, but much higher than Group II oils (Figure 5 and Table 3). The ratio of 1-cage adamantanes to 2-cage diamantanes is 0.54–1.25 (Averaged 0.90) for Group I oils, 3.04–27.55 (Averaged 12.8) for Group III oils and 8.80–35.07 (Averaged 18.8) for Group IV oils, indicating the higher contribution of adamantanes to diamondoids for Group III/IV oils than Group I oils (Figure 5).

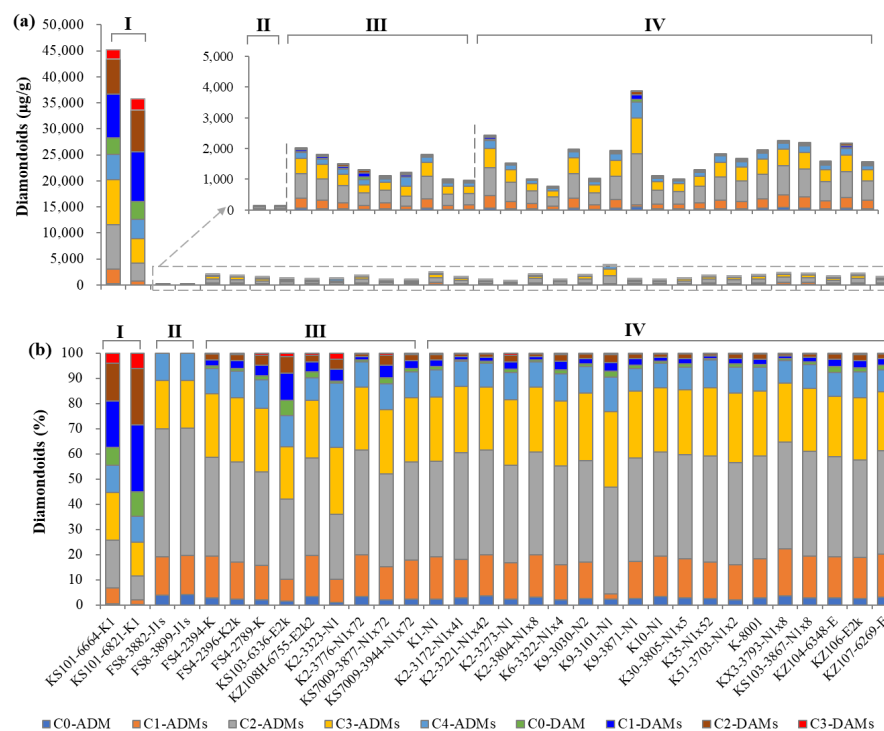


Figure 5. The (a) absolute and (b) relative concentrations of diamondoids in oils from the Kekeya area, I–IV indicate the oil groups.

Table 3. Molecular parameters and concentrations of diamondoids for crude oil samples collected from the Kekeya area.

Oil Group	Well	Depth (m)	Formation	MAI	MDI	%Ro	ADMs/ DAMs	C ₀ - ADM (µg/g)	C ₁ - ADM (µg/g)	C ₂ - ADM (µg/g)	C ₃ - ADM (µg/g)	C ₄ - ADM (µg/g)	C ₀₋₄ - ADMs (µg/g)	C ₀ - DAM (µg/g)	C ₁ - DAM (µg/g)	C ₂ - DAM (µg/g)	C ₃ - DAM (µg/g)	C ₀₋₃ - DAMs (µg/g)	Diamondoids (µg/g)
Group I	KS101	6664	K ₁	0.84	0.60	1.89	1.25	214	2813	8598	8567	4922	25113	3164	8361	6765	1842	20,132	45,244
		6821	K ₁	0.77	0.59	1.87	0.54	37	703	3411	4732	3667	12549	3495	9483	8020	2216	23,214	35,763
Group II	FS8	3882	J _{1s}	0.64	0.00	n.a	n.a	6	22	75	29	16	147	n.a	n.a	n.a	n.a	n.a	147
		3899	J _{1s}	0.67	0.00	n.a	n.a	6	23	75	28	16	148	n.a	n.a	n.a	n.a	n.a	148
Group III	FS4	2394	K ₂	0.70	0.33	1.23	15.43	58	328	785	507	202	1879	18	52	43	9	122	2001
	FS4	2396	K ₂	0.68	0.36	1.32	13.02	40	267	711	459	189	1665	18	54	46	9	128	1793
	FS4	2789	K ₂	0.68	0.35	1.30	8.46	31	204	552	376	168	1331	23	64	57	14	157	1488
	KS103	6336	E _{2k}	0.60	0.32	1.22	3.04	20	115	414	273	163	984	79	142	86	18	324	1308
	KZ108H	6755	E _{2k} ₂	0.73	0.39	1.39	9.19	37	183	429	257	98	1003	25	45	30	9	109	1113
	K2	3323	N ₁	0.66	0.45	1.53	7.75	13	112	314	323	313	1074	6	61	48	28	144	1218
	K2	3776	N _{1x7} ²	0.72	0.40	1.42	27.55	57	298	741	444	177	1718	12	25	20	5	62	1780
	KS7009	3877	N _{1x7} ²	0.69	0.50	1.65	7.26	21	129	366	255	103	874	22	51	40	9	120	994
KS7009	3944	N _{1x7} ²	0.70	0.36	1.30	12.36	23	145	367	240	97	871	14	28	24	5	70	941	
Group IV	K1	/	N ₁	0.78	0.42	1.47	14.04	58	407	918	618	263	2264	33	65	52	12	161	2425
	K2	3172	N _{1x4} ¹	0.71	0.39	1.38	29.93	43	230	637	398	149	1456	8	21	17	4	49	1505
	K2	3221	N _{1x4} ²	0.71	0.37	1.33	23.96	35	163	415	248	95	956	8	15	13	4	40	996
	K2	3273	N ₁	0.70	0.32	1.21	12.14	18	108	293	196	83	698	10	22	19	7	58	755
	K2	3804	N _{1x8}	0.73	0.35	1.30	27.81	61	327	802	503	198	1892	13	29	21	5	68	1960
	K6	3322	N _{1x4}	0.68	0.36	1.32	11.05	20	143	396	261	110	930	16	34	27	7	84	1014
	K9	3030	N ₂	0.71	0.33	1.25	17.33	49	280	777	516	201	1821	22	44	33	7	105	1926
	K9	3101	N ₁	0.71	0.39	1.38	8.80	91	77	1650	1168	527	3514	89	141	114	27	371	3884
	K9	3871	N ₁	0.70	0.34	1.27	15.69	29	160	449	292	99	1028	14	26	20	5	66	1094
	K10	/	N ₁	0.71	0.32	1.22	24.19	33	157	408	251	96	945	7	15	13	3	39	984
	K30	3805	N _{1x5}	0.71	0.33	1.24	17.12	35	204	534	331	117	1221	14	28	24	5	71	1293
	K35	/	N _{1x5} ²	0.68	0.36	1.31	35.07	44	264	761	487	198	1754	11	19	15	5	50	1804
	K51	3703	N _{1x2}	0.69	0.36	1.31	17.29	33	231	674	456	173	1566	19	37	28	7	91	1657
	K8001	3929	N _{1x8}	0.72	0.38	1.37	16.86	53	307	794	505	186	1845	21	43	38	8	109	1954
	KX3	3793	N _{1x8}	0.76	0.39	1.38	32.29	82	417	949	525	201	2172	17	24	22	5	67	2240
	KS103	3867	N _{1x8}	0.72	0.38	1.36	20.90	61	363	910	548	206	2087	23	39	32	6	100	2187
KZ104	6348	E	0.72	0.40	1.41	12.21	46	258	627	378	152	1460	34	46	34	6	120	1580	
KZ106	/	E _{2k}	0.68	0.36	1.32	12.23	54	352	839	535	217	1997	37	64	51	12	163	2161	
KZ107	6269	E	0.73	0.38	1.36	14.29	46	266	634	357	138	1441	28	39	30	5	101	1542	

Note: MAI = 1-methyladamantane/(1-methyladamantane + 2-methyladamantane); MDI = 4-methyldiamantane/(1-methyldiamantane + 3-methyldiamantane + 4-methyldiamantane); %Ro = 2.4322 × MDI + 0.4389; ADMs/DAMs: the total concentration ratio of adamantanes to diamantanes; ADM: adamantane; DAM: diamantane.

3.4. Aromatic Compounds

Naphthalenes, phenanthrenes, dibenzothiophenes and triaromatic steranes are the major components of aromatic compounds in crude oils from the Kekeya area (Figure 6). Several differences in molecular compositions can be observed among various group oils (Figures 6 and 7). Group I oils are extremely enriched in aromatic compounds (62,966–228,944 $\mu\text{g/g}$), in particular phenanthrenes (22,478–47,204 $\mu\text{g/g}$) and dibenzothiophenes (5500–12,032 $\mu\text{g/g}$) relative to the others. Compared with Group I oils, Group II oils contains more triaromatic steranes (133–144 $\mu\text{g/g}$) with the lowest $\text{TA}[\text{C}_{20}/(\text{C}_{20} + \text{C}_{28})-20\text{R}]$ value of 0.32–0.33, and much less phenanthrenes (734–810 $\mu\text{g/g}$) and dibenzothiophenes (20–28 $\mu\text{g/g}$). Group III/IV oils are depleted in triaromatic steranes (<12 $\mu\text{g/g}$) but with the greater $\text{TA}[\text{C}_{20}/(\text{C}_{20} + \text{C}_{28})-20\text{R}]$ ratio of 0.62–0.82 and present large variations in the absolute concentrations of the other aromatic compounds. For example, phenanthrenes are 209–1893 $\mu\text{g/g}$ for Group III oils and 206–1606 $\mu\text{g/g}$ for Group IV oils, dibenzothiophenes are 5–297 $\mu\text{g/g}$ for Group III oils and 1–369 $\mu\text{g/g}$ for Group IV oils (Table 4).

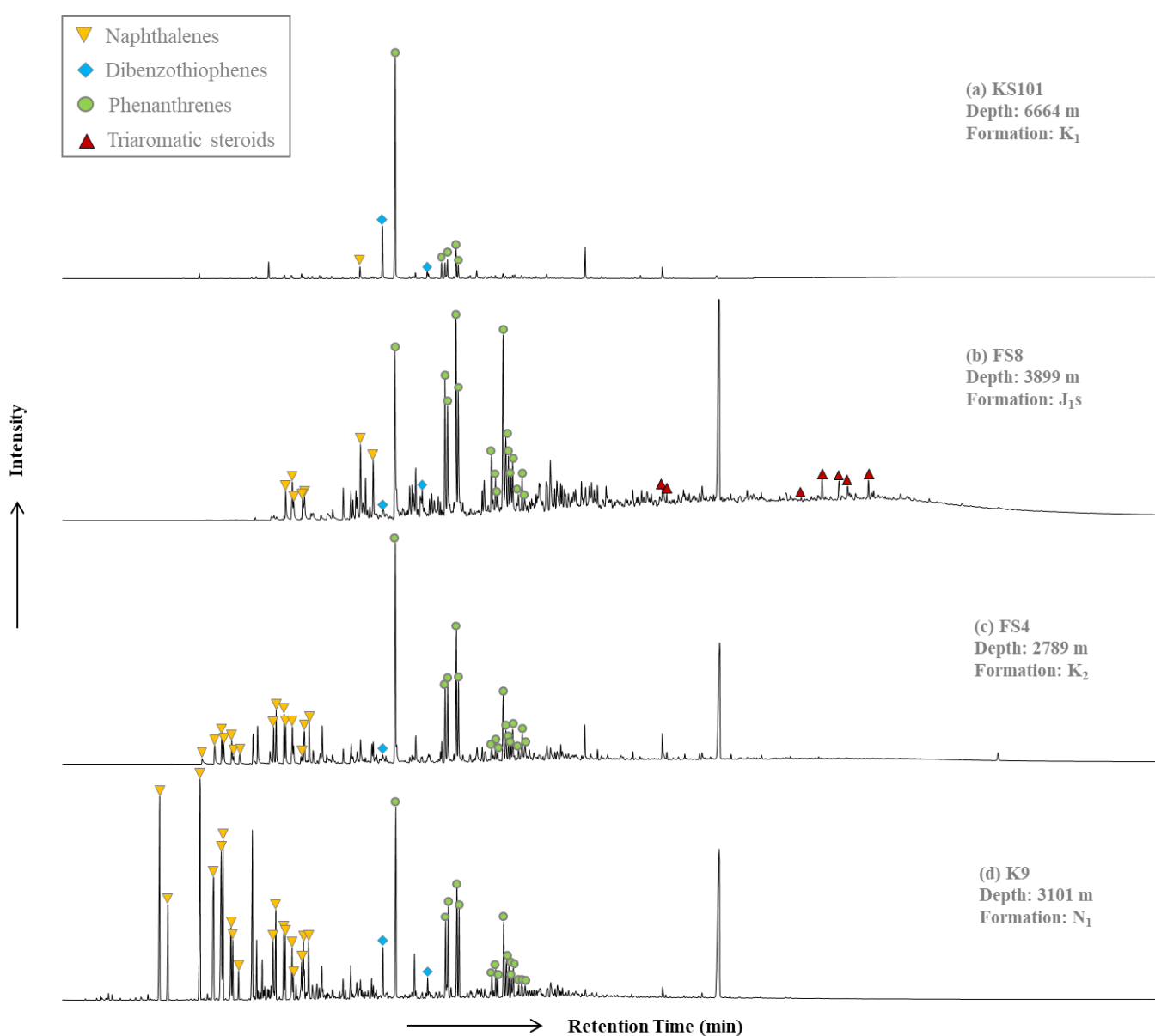


Figure 6. Typical total ion chromatography of aromatic fraction for oils from the Kekeya area.

Table 4. Molecular parameters and concentrations of aromatics for crude oils from the Kekeya area.

Oil Group	Well	Depth (m)	Formation	Naphthalenes (µg/g)	Phenanthrenes (µg/g)	Dibenzothiophenes (µg/g)	Triaromatic Steroids (µg/g)	Aromatics (µg/g)	DNR	MPI ₁	MPI ₂	MPR	MDR	DBT/P	TA[C ₂₀ /(C ₂₀ + C ₂₈)-20R]
Group I	KS101	6664	K ₁	941	22,478	5500	25	28,944	1.87	0.14	0.16	0.76	4.09	0.23	0.55
		6821	K ₁	3696	47,204	12,032	34	62,966	4.59	0.13	0.14	0.77	4.86	0.25	0.69
Group II	FS8	3882	J _{1s}	1253	734	20	133	2140	1.89	0.57	0.54	0.80	5.65	0.01	0.33
		3899	J _{1s}	293	810	28	144	1275	1.36	0.59	0.57	0.84	5.05	0.02	0.32
Group III	FS4	2394	K ₂	875	1372	68	12	2327	3.32	0.39	0.39	0.73	7.02	0.04	0.62
	FS4	2396	K ₂	745	1327	71	10	2153	1.55	0.43	0.46	0.78	8.15	0.04	0.66
	FS4	2789	K ₂	977	1893	100	9	2979	1.98	0.38	0.41	0.73	7.70	0.05	0.65
	KS103	6336	E _{2k}	195	1215	82	0	1492	0.75	0.47	0.49	0.58	3.42	0.09	/
	KZ108H	6755	E _{2k} ₂	8	209	5	0	222	1.75	0.82	1.05	0.80	2.54	0.04	/
	K2	3323	N ₁	2575	824	163	3	3565	9.23	0.39	0.44	0.68	1.22	0.19	0.71
	K2	3776	N _{1x7} ²	2265	595	11	0	2871	3.60	0.38	0.41	0.76	4.19	0.03	/
	K10	/	N ₁	2279	585	11	0	2875	3.80	0.41	0.44	0.76	4.04	0.03	/
	KS7009	3877	N _{1x7} ²	1209	1252	297	8	2766	3.65	0.41	0.44	0.67	1.25	0.26	0.81
	KS7009	3944	N _{1x7} ²	18	1205	188	4	1415	1.20	0.44	0.47	0.71	1.27	0.17	0.76
Group IV	K1	/	N ₁	339	621	28	1	989	6.80	0.55	0.62	0.72	2.03	0.03	0.64
	K2	3172	N _{1x4} ¹	2441	471	12	0	2924	3.68	0.37	0.41	0.70	0.62	0.03	/
	K2	3221	N _{1x4} ²	2059	1045	239	0	3343	10.17	0.40	0.43	0.65	1.17	0.25	/
	K2	3273	N ₁	50	839	111	2	1002	1.37	0.42	0.47	0.68	1.26	0.09	0.73
	K2	3804	N _{1x8}	28	206	1	0	235	2.48	0.51	0.59	0.83	/	0.01	/
	K6	3322	N _{1x4}	156	1192	210	0	1558	0.76	0.43	0.47	0.67	1.21	0.17	/
	K9	3030	N ₂	55	736	107	2	900	2.14	0.41	0.44	0.74	1.47	0.11	0.74
	K9	3101	N ₁	2575	1606	329	0	4510	3.76	0.46	0.49	0.79	1.63	0.25	/
	K9	3871	N ₁	52	963	126	1	1142	1.30	0.47	0.50	0.79	1.62	0.11	0.79
	K30	3805	N _{1x5}	1916	1016	192	0	3124	5.59	0.45	0.46	0.72	1.43	0.22	/
	K35	/	N _{1x5} ²	2575	643	145	0	3363	4.18	0.43	0.46	0.80	1.34	0.25	/
	K51	3703	N _{1x2}	1951	522	103	0	2576	3.53	0.41	0.43	0.74	1.43	0.23	/
	K8001	3929	N _{1x8}	769	1180	236	0	2185	16.34	0.46	0.48	0.79	1.81	0.24	/
	KX3	3793	N _{1x8}	1544	701	73	0	2318	6.57	0.42	0.44	0.80	1.47	0.13	/
	KS103	3867	N _{1x8}	53	927	128	3	1111	/	0.46	0.48	0.79	1.65	0.12	0.82
	KZ104	6348	E	127	293	3	0	423	/	0.92	1.10	0.87	2.13	0.02	/
	KZ106	/	E _{2k}	919	1160	220	0	2299	3.01	0.48	0.50	0.77	1.69	0.23	/
KZ107	6269	E	7	556	19	0	582	/	0.65	0.71	0.82	2.54	0.02	/	

Note: DNR = (2,6-dimethylnaphthalene + dimethylnaphthalene)/1,5-dimethylnaphthalene; MPI₁ = 1.5 × (2-methylphenanthrene + 3-methylphenanthrene)/(phenanthrene + 1-methylphenanthrene + 9-methylphenanthrene); MPI₂ = 3 × (2-methylphenanthrene)/(phenanthrene + 1-methylphenanthrene + 9-methylphenanthrene); MPR = (3-methylphenanthrene + 2-methylphenanthrene)/(9-methylphenanthrene + 1-methylphenanthrene); MDR = 4-methyldibenzothiophene /1-methyldibenzothiophene; TA: Triaromatic; /: The content is too low to be detected.

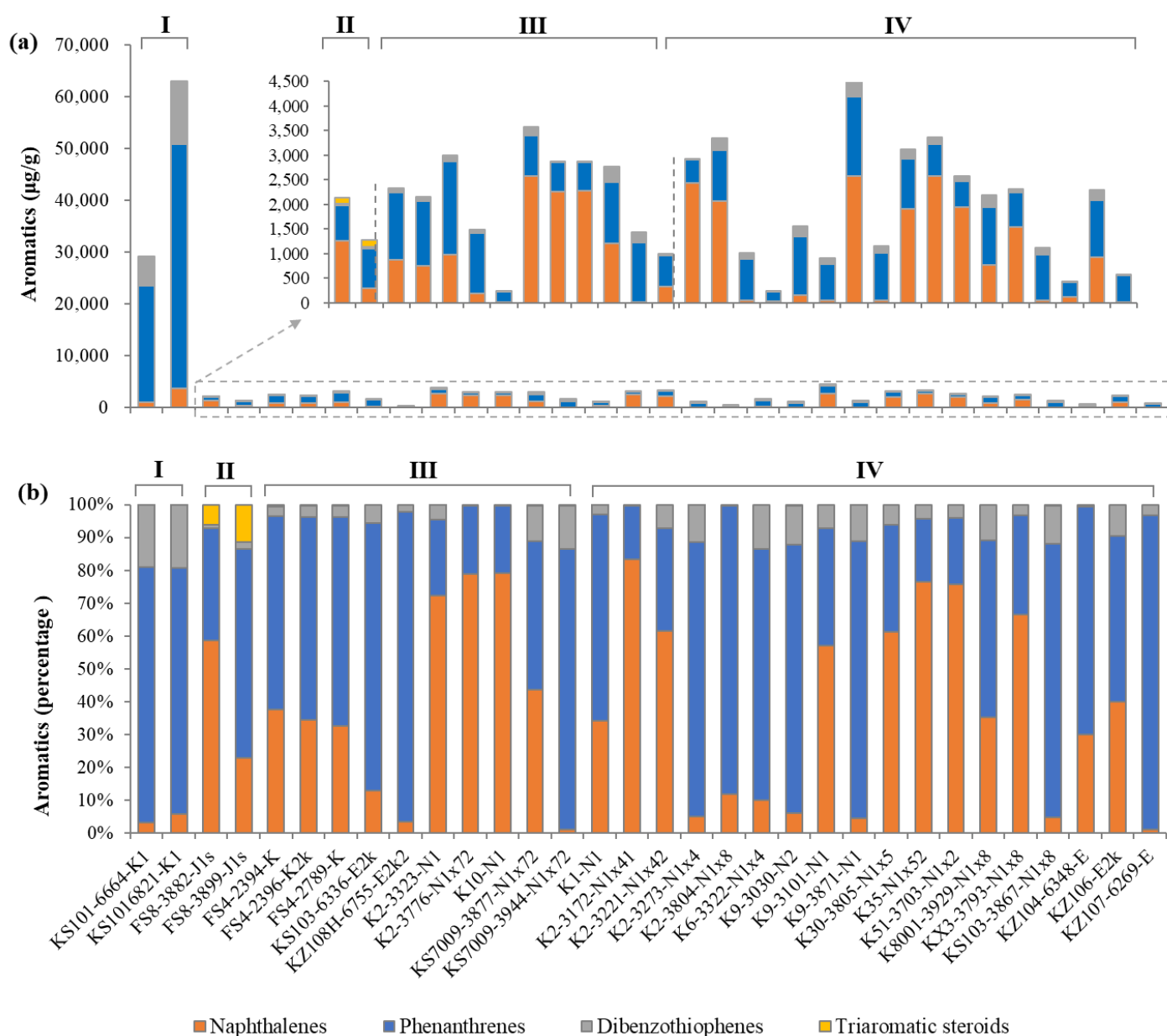


Figure 7. The (a) absolute and (b) relative concentrations of aromatics for oils in the Kekeya area, I–IV indicate the oil groups.

3.5. Carbon Isotopic Composition of Individual *n*-Alkanes for Crude Oils

Table 5 presents the $\delta^{13}\text{C}$ values of whole oils and individual *n*-alkanes for crude oils from the Kekeya area. Group I oils are relatively ^{13}C -enriched in the whole oil by presenting around 4% heavier than Group II oils, and 2% heavier than Group III/IV oils (Table 5). This is consistent with the distribution patterns of $\delta^{13}\text{C}$ values of individual *n*-alkanes.

The $\delta^{13}\text{C}$ values of individual *n*-alkanes for all samples present a decreasing pattern with carbon number increasing. They extend from -30.2% to -26.1% for Group I oils, -32.1% to -29.8% for Group II oils and -32.4% to -27.6% for Group III/IV oils (Figure 8 and Table 5). The $\delta^{13}\text{C}$ values of individual *n*-alkanes for Group I oils are 2–4% heavier than that for Group II oils, and around 2% heavier than that for Group III/IV oils.

Table 5. The $\delta^{13}\text{C}$ values of whole oil and individual *n*-alkanes for oil samples collected from the Kekeya area.

Oil Group	Well	Depth (m)	Formation	$\delta^{13}\text{C}_{\text{oil}}$ (%)	<i>n</i> -C ₁₂	<i>n</i> -C ₁₃	<i>n</i> -C ₁₄	<i>n</i> -C ₁₅	<i>n</i> -C ₁₆	<i>n</i> -C ₁₇	<i>n</i> -C ₁₈	<i>n</i> -C ₁₉	<i>n</i> -C ₂₀	<i>n</i> -C ₂₁	<i>n</i> -C ₂₂	<i>n</i> -C ₂₃	<i>n</i> -C ₂₄	<i>n</i> -C ₂₅	<i>n</i> -C ₂₆	<i>n</i> -C ₂₇	<i>n</i> -C ₂₈	<i>n</i> -C ₂₉	<i>n</i> -C ₃₀	<i>n</i> -C ₃₁	<i>n</i> -C ₃₂	
Group I	KS101	6664	K ₁	-27.7	-27.8	-28	-28.6	-28.9	-29	-29.2	-29.5	-29.5	-29	-29.5	-29.8	-30.2	-29.5	-30.2	-29.8	-29.3	-29.5	-29	-29.1	-29.6	/	
		6821	K ₁	-26.9	-26.1	-26.5	-27.3	-27.3	-27.8	-28	-28.3	-27.4	-28.2	-27.9	-28.1	-28.3	-27.9	-28.9	-28.4	-28.9	-27.9	-28.1	-28	-28.2	-28.2	-28.6
Group II	FS8	3882	J _{1s}	-28.9	-30.1	-30.5	-30	-30.6	-30.6	-30.4	-30	-32	-31.5	-31.9	-31.6	-31.5	-31.4	-31.6	-31.5	-31.8	-31.4	-31.1	-31	-30.8	-30.7	
		3899	J _{1s}	-28.6	-30.4	-30.2	-30.1	-30.1	-30.1	-30.1	-30.5	-29.8	-31.3	-31.6	-32.1	-31.3	-31.9	-31.6	-31.5	-31.7	-31.4	-30.8	-31.3	-31.1	-30.8	-30.2
Group III	KS103	2394	K ₂	-30.8	-28.4	-28.6	-28.9	-29.3	-28.9	-29	-28.7	-30.1	-29.8	-30	-30.1	-29.8	-30.1	-30.5	-30.2	-30.7	-30.8	-30.8	-30.8	-30.8	-30.4	-30.4
		2396	K ₂	-28.1	-29.2	-29.3	-29.1	-29.7	-29.7	-29.5	-30	-30	-29.6	-29.8	-30.1	-30.6	-30.6	-30.3	-30.9	-31.2	-30.7	-30.5	-30.3	-31.1	-30.3	-31.1
		2789	K ₂	-28.9	-29.2	-29.9	-29.4	-29.9	-29.6	-29.2	-29	-30	-30.1	-29.3	-30	-30.5	-30.3	-30.6	-30.6	-30.9	-30.1	-29.3	-30.7	-29.2	/	/
		6336	E _{2k}	-29.8	-29.7	-29.7	-29.8	-30.3	-29.8	-29.9	-29.3	-30	-30.7	-31.3	-30.9	-31.2	-30.8	-30.9	-31.4	-31.4	-31.4	-31.4	-31.7	-30.7	-30.9	-30.5
		6755	E _{2k2}	-29.1	-29.2	-29	-29.5	-29.7	-29.6	-30.2	-29.6	-29.9	-30.2	-30.7	-30.5	-30.9	-30.2	-30.7	-31.2	-31.4	-31	-31	-30.5	/	/	/
		3323	N ₁	-29.8	-29.1	-28.7	-29	-29.5	-29.7	-29.7	-30.5	-30.1	-30.3	-30.8	-31.2	-30.7	-31.2	-31.4	/	/	/	/	/	/	/	/
		3776	N _{1x7} ²	-29.5	-29.2	-29	-29.5	-30	-29.4	-29.7	-29.2	-30.7	-30.5	-30.9	-30.8	-30.8	-30.4	-31.3	-31.2	-31.4	-31.4	-31	-31.2	-30.9	-30.3	-30.3
		/	N ₁	-27.7	-27.8	-28	-28.5	-29.1	-28.9	-29.1	-29.2	-30.1	-29.8	-30.7	-30.8	-30.9	-30.4	-30.6	-31.5	-31.3	-32.4	/	/	/	/	/
		3877	N _{1x7} ²	-29.6	-29.1	-29.2	-29	-29.6	-29.4	-29.3	-29.7	-30.5	-30.3	-30.7	-30.4	-30.7	-30.9	-31.1	-30.8	-31	-31.1	-31.2	-30.3	-30.4	-30.7	-30.7
		3944	N _{1x7} ²	-28.9	-29.1	-29.1	-29.4	-29.8	-29.2	-29.4	-29.2	-29.8	-30.3	-30.8	-30.4	-30.7	-30.4	-31.2	-31.2	-31.2	-31.5	-30.9	-31.1	-30.4	-30.2	-29.9
Group IV	KS7009	/	N ₁	-29.2	-28.7	-28.7	-29.1	-29.7	-29.3	-29.5	-29.6	-30.2	-30.1	-30.4	-30.4	-31.2	-30.9	-30.9	-31.8	-32.1	-31.5	-31.4	-31.8	/	/	
		3172	N _{1x4} ¹	-29.6	-27.6	-28.3	-28.2	-28.9	-29.3	-29.7	-29.1	-30.3	-29.8	-30.7	-30.6	-30.5	-30.4	-30.6	-31.3	-31.3	-31.5	-31.4	-31.1	/	/	
		3221	N _{1x4} ²	-29.2	-29.1	-29.2	-29.6	-29.8	-29.9	-29.6	-29.4	-30.4	-29.9	-30.5	-30.9	-30.3	-30.3	-31.4	-31	-31	-31.1	-30.3	/	/	/	
		3273	N ₁	-29.1	-28.8	-29.1	-29.5	-29.6	-29.4	-29.3	-29.9	-30.6	-30.3	-30.2	-30.9	-30.3	-31.3	-31	-30.8	-30.9	-31.3	-30.7	-30.6	-30.4	-30.4	
		3804	N _{1x8}	-29.2	-28.6	-28.7	-29.1	-29.6	-29.4	-29.2	-29	-29.9	-30	-30.6	-30.5	-30.1	-30.6	-30.8	-30.8	-31.5	-31.4	-31.3	-31.3	-30.3	-29.7	
		3322	N _{1x4}	-29.6	-29.1	-28.9	-29.2	-29.8	-29.4	-29.8	-29.6	-30.3	-30.1	-30.7	-31.2	-31.1	-30.9	-31.4	-31.6	-32.1	-31.4	-31.7	-31.6	-30.9	-30.9	
		3030	N ₂	-27.9	-28.4	-28.5	-28.5	-29.3	-29	-29.7	-28.9	-30.6	-30.1	-30.6	-30.4	-31	-30.5	-31.5	-31.6	-31.7	-32	-32	-31	/	/	
		3101	N ₁	-29.5	-28.8	-28.8	-29.1	-29.7	-29.4	-29.4	-29.1	-30.7	-30	-30.8	-30.5	-30.7	-30.9	-31.2	-30.9	-31.2	-31.2	-31.9	-30.9	-30.6	-30.1	
		3871	N ₁	-29.8	-28.6	-28.8	-29.8	-29.7	-29.3	-29.9	-29.5	-30.8	-30.6	-31	-30.9	-31.1	-30.6	-31.7	-31.5	-32.4	-32.1	-32.3	-31.2	-31.1	-31.1	
		3805	N _{1x5}	-29.6	-27.6	-28.3	-28.3	-29.3	-29.2	-29.2	-28.9	-30.1	-29.5	-30.4	-30.4	-30.7	-30.3	-31.2	-31.4	-31.7	-31.8	-31.6	-31	-31.2	-29.2	
		/	N _{1x5} ²	-29.4	-28.9	-29.2	-29.1	-29.7	-29.6	-30	-29.5	-30.5	-30.7	-30.4	-30.8	-31.4	-30.7	/	/	/	/	/	/	/	/	
		3703	N _{1x2}	-29.4	-28.7	-28.8	-29	-29.9	-29.6	-29.4	-29.3	-30.3	-30.2	-30.9	-30.7	-31.4	-31	-31.3	-31.4	-31.5	-31.7	-31.2	/	/	/	
		3929	N _{1x8}	-29.6	-27.9	-28.2	-28.4	-29.2	-29.1	-29.3	-28.9	-29.8	-30.3	-30.3	-30.8	-30.5	-31.1	-31.6	-32	-32.1	-32.3	-31.2	-31.2	-31.6	/	
		3793	N _{1x8}	-29.2	-28.4	-29	-29.5	-29.9	-29.4	-29.8	-30	-30.6	-29.7	-30.1	-30.5	-30.9	-30.7	-31.4	-32.1	-31.3	-31.9	/	/	/	/	
		3867	N _{1x8}	-27.6	-28.2	-28.3	-28.4	-29.3	-29.2	-29.1	-29.3	-30.3	-29.6	-29.6	-30.4	-30.9	-30.8	-30.8	-31.5	-31.6	-31.6	-32.3	-31.1	/	/	
		6348	E	-29.4	-27.8	-28	-28.6	-28.9	-29	-29.2	-29.5	-29.5	-29	-29.5	-29.8	-30.2	-29.5	-30.2	-29.8	-29.3	-29.5	-29	-29.1	-29.6	/	
		/	E _{2k}	-29.4	-26.1	-26.5	-27.3	-27.3	-27.8	-28	-28.3	-27.4	-28.2	-27.9	-28.1	-28.3	-27.9	-28.9	-28.4	-28.9	-27.9	-28.1	-28	-28.2	-28.6	
/	E	-29.3	-30.1	-30.5	-30	-30.6	-30.6	-30.4	-30	-32	-31.5	-31.9	-31.6	-31.5	-31.4	-31.6	-31.5	-31.8	-31.1	-31.1	-31	-30.8	-30.7			

Note: /: The content is too low to be detected.

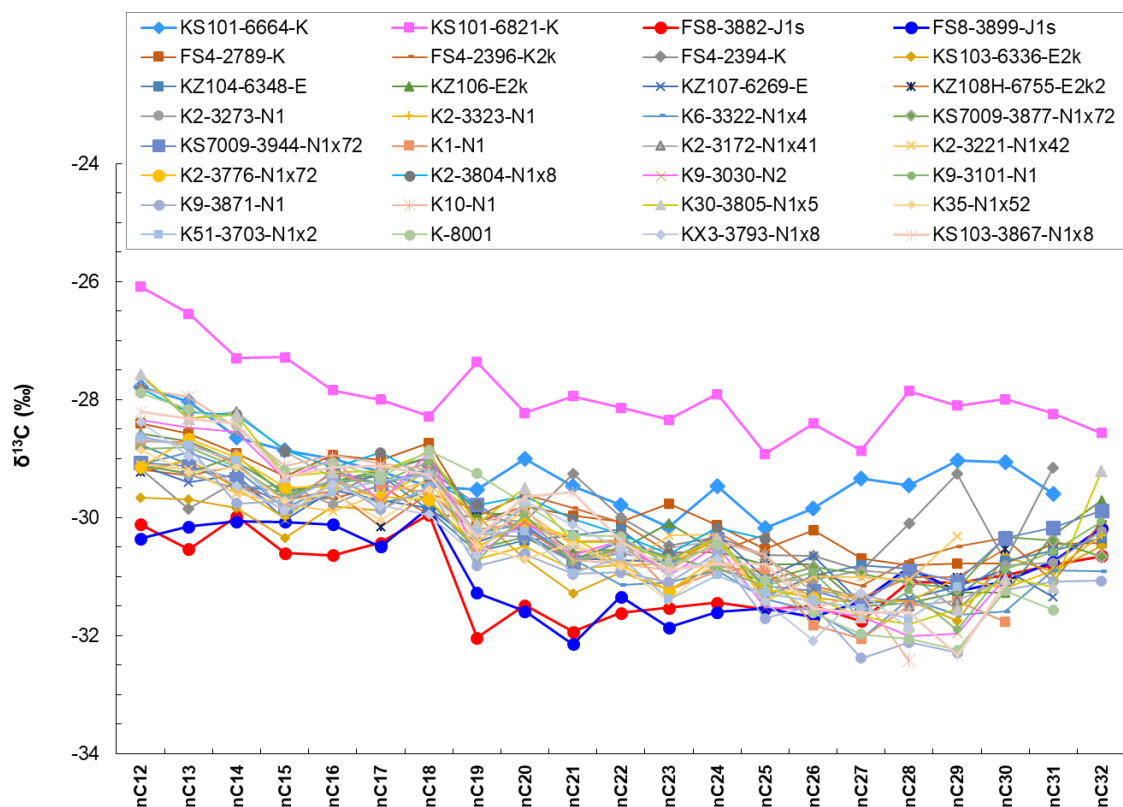


Figure 8. Stable carbon isotope profiles for oils collected from the Kekeya area.

4. Discussion

4.1. Depositional Environments and Organic Matter Inputs of Oil Sources

Molecular biomarkers in the saturated and aromatic fractions of collected oil samples can be used to constraint the depositional environments and organic matter inputs of source rocks [24]. The ratios of Pr/*n*-C₁₇ and Ph/*n*-C₁₈ are 0.06–0.16 and 0.04–0.10, respectively (Table 2). On the crossplots of Pr/*n*-C₁₇ versus Ph/*n*-C₁₈ most oils are located at the area of mixed Type II/III organic matter (Figure 9a). This indicates that petroleum source rocks were deposited under the suboxidized conditions with the mixed inputs of terrigenous higher plants and aquatic algae [25–27].

The ratios of Pr/Ph and DBT/PHEN for these oil samples are 1.02–1.84 and 0.01–0.26, respectively (Tables 2 and 4). On the crossplots of Pr/Ph versus DBT/PHEN, these oils are located at the area of marine shale and other lacustrine shales (Figure 9b). This indicates that petroleum source rocks were deposited under the lacustrine settings [28], which is consistent with the previous investigations [3,29]. Specifically, during the middle-to-late Early Permian period, the southwest depression experienced the crustal uplift from east to west. The Permian Pusige Formation was deposited under the lacustrine setting in the Kekeya area. During the Jurassic period, the faulted subsidence occurred with the water depth increasing gradually from the foreland area to the depression, the faulted lacustrine sedimentary system was developed in Kekeya area [30,31]. The predominance of C₂₁TT among tricyclic terpanes further indicates that lacustrine algae act as the major contributor to organic matters within the source rocks [32,33].

Terrestrial higher plants may have a greater contribution to the source rocks for Group II oils. C₂₄ Tetracyclic terpenane is considered to be originated from higher plants and C₂₆ Tricyclic terpanes are assumed to be generated from aquatic organisms [34,35]. The ratio of C₂₄Ter/C₂₆TT can be used to evaluate the relative inputs of terrestrial higher plants and aquatic algae [34]. It is relatively higher for Group II oils (Table 1). C₂₇ regular steranes are generated from aquatic organisms and algae [36,37], C₂₈ regular steranes are derived from diatoms, coccolithophores, and dinoflagellates, and C₂₉ regular steranes are originated

from algae and terrestrial higher plants [24,38]. The ratios of C_{29} -/ C_{27} -regular steranes and C_{29} $\alpha\alpha\alpha 20R$ / C_{27} $\alpha\alpha\alpha 20R$ and the concentrations of C_{29} -regular steranes are both higher for Group II oils than those for the other oils (Figure 9c,d). This indicates that terrestrial higher plants have a greater contribution to the source rocks for Group II oils [39], which may be caused by the more oxidized depositional environments as indicated by the greater Pr/Ph ratio (Table 2).

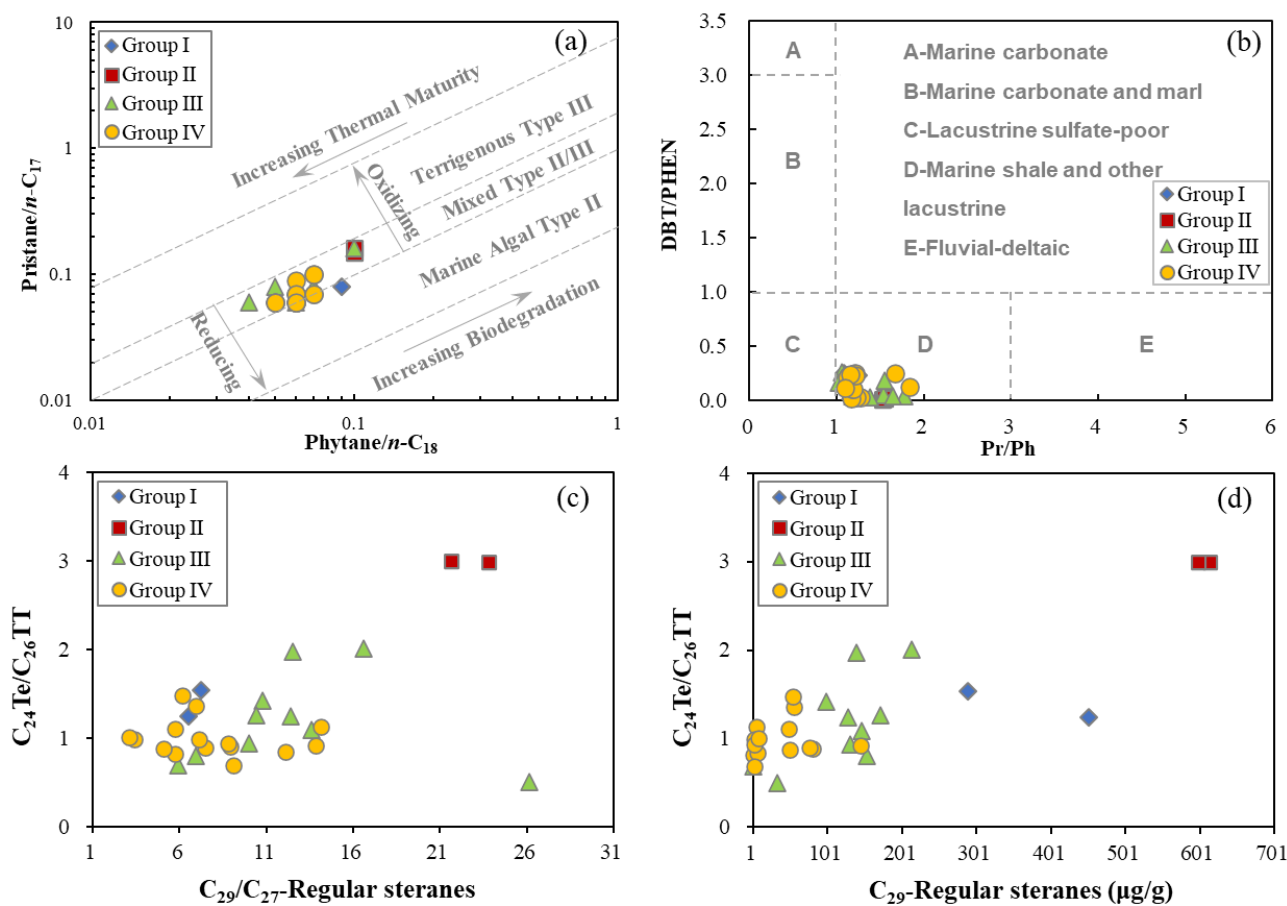


Figure 9. The crossplots of biomarker parameters referring to depositional environments and organic matter inputs for oil sources in the Kekeya area. (a) Pr/ n - C_{17} versus Ph/ n - C_{18} ; (b) Pr/Ph versus DBT/PHEN; (c) C_{29} / C_{27} -Regular steranes versus $C_{24}Te/C_{26}TT$; (d) C_{29} Regular steranes ($\mu\text{g/g}$) versus $C_{24}Te/C_{26}TT$.

4.2. Thermal Maturity of Crude Oils and Hydrocarbon Mixing

Hopanes and steranes indicate matured oils in the study area. The cross-plot of C_{29} $\beta\beta/(\alpha\alpha + \beta\beta)$ versus C_{29} $\alpha\alpha\alpha$ -20S/(20S + 20R) suggests matured oils, while these two ratios for Group I/II oils are relatively lower, indicating lower thermal maturity levels relative to Group III/IV oils (Figure 10a). The C_{29} 20S/(20S + 20R) ratio mostly ranges from 0.50 to 0.55 for Group III/IV oils (Table 1), approaching the equilibrium value (0.52–0.55) [40]. Therefore, care should be taken to this isomerization ratio. The C_{29} $\beta\beta/(\beta\beta + \alpha\alpha)$ ratio is independent of source organic matter inputs and 0.50–0.58 for Group III/IV oils, which does not approach the equilibrium value (0.67–0.72) [25,41]. The positive correlation between C_{29} $\beta\beta/(\beta\beta + \alpha\alpha)$ and Ts/(Ts + Tm) suggests that Ts/(Ts + Tm) is significantly affected by thermal stress rather than organic facies (Figure 10b). The Ts/(Ts + Tm) ratio also indicates more matured oils for Group III/IV (Equivalent %Ro = 0.9–1.3) than Group I/II (Equivalent %Ro = 0.6–0.8) [40]. The positive relations between Ts/(Ts + Tm) and dia $C_{30}H/C_{30}H$ and dia $C_{30}H/C_{29}$ Ts and TA [$C_{20}/(C_{20} + C_{28})$ -20R] highlight the dominated role of ther-

mal stress on molecular compositions and associated parameters (Figure 10c–e) [42,43], resulting in the different distribution patterns of terpanes and steranes (Figure 3).

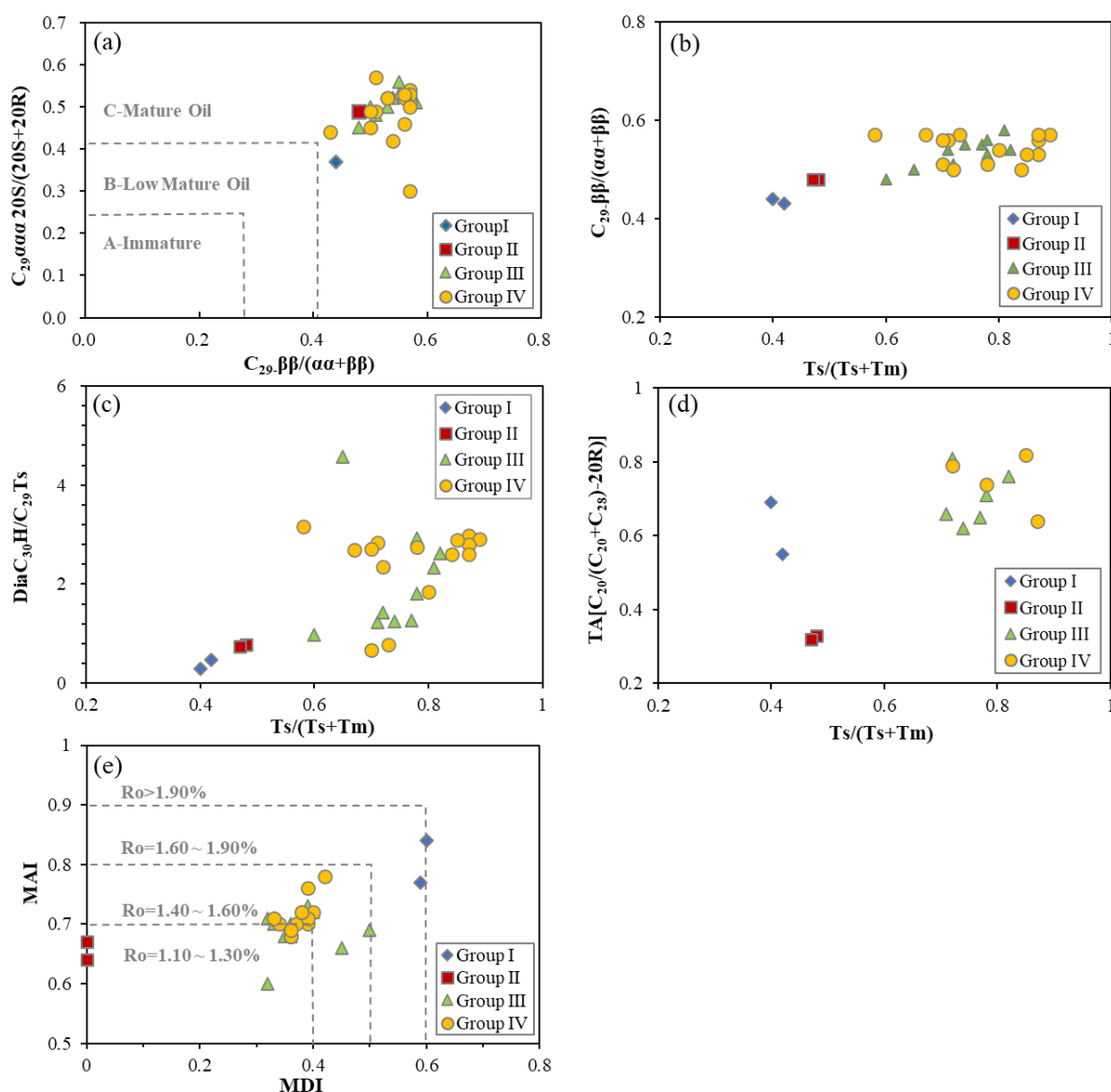


Figure 10. The crossplots of thermal maturity parameters for crude oils from the Kekeya area. (a) $C_{29}\text{-}\beta\beta/(\alpha\alpha + \beta\beta)$ versus $C_{29}\text{-}\alpha\alpha\alpha 20S/(20S + 20R)$; (b) $Ts/(Ts + Tm)$ versus $C_{29} \beta\beta/(\alpha\alpha + \beta\beta)$; (c) $Ts/(Ts + Tm)$ versus $\text{dia}C_{30}H/C_{29} Ts$; (d) $Ts/(Ts + Tm)$ versus $TA [C_{20}/(C_{20} + C_{28})\text{-}20R]$; (e) MAI versus MDI.

Adamantanes and diamantanes indicate more matured oils. Due to less thermal stability relative to diamondoids, terpanes, steranes and triaromatic steranes decrease subsequently from Group I to IV, and diamondoids show the opposite trend (Figure 11a–f). The increasing concentrations of diamondoids indicate the increased thermal maturity levels from Group II to IV oils. This is further confirmed by the parameters of MAI and MDI for diamondoids [44]. The crossplot of MDI versus MAI indicates that the equivalent %Ro is generally 1.1–1.3 for Group II oils, 1.3–1.6 for Group III/IV oils and 1.6–1.9 for Group I oils (Figure 10e). The $C_{19}\text{-}C_{23}TT/C_{30}H$ ratio presents the positive correlations with adamantanes and diamantanes (except for Group I oils) (Figure 11g,h), indicating thermal stress has the critical role in regulating the evolution path of this parameter.

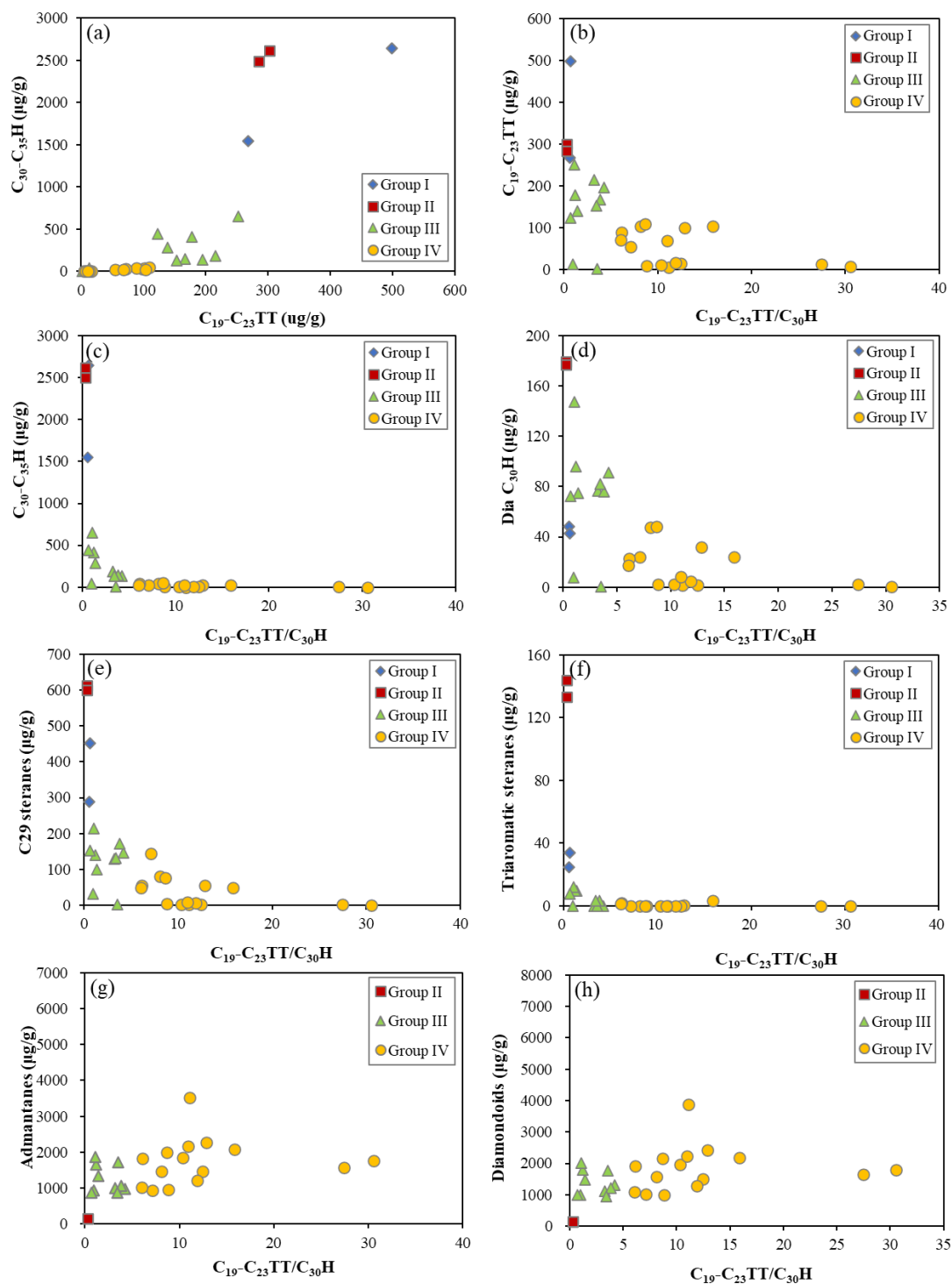


Figure 11. The crossplots of molecular parameters and absolute concentrations for crude oils from the Kekeya area. (a) $C_{19}\text{-}C_{23}\text{TT}$ ($\mu\text{g/g}$) versus $C_{30}\text{-}C_{35}\text{H}$ ($\mu\text{g/g}$); (b) $C_{19}\text{-}C_{23}\text{TT}/C_{30}\text{H}$ versus $C_{19}\text{-}C_{23}\text{TT}$ ($\mu\text{g/g}$); (c) $C_{19}\text{-}C_{23}\text{TT}/C_{30}\text{H}$ versus $C_{30}\text{-}C_{35}\text{H}$ ($\mu\text{g/g}$); (d) $C_{19}\text{-}C_{23}\text{TT}/C_{30}\text{H}$ versus Dia $C_{30}\text{H}$; (e) $C_{19}\text{-}C_{23}\text{TT}/C_{30}\text{H}$ versus C_{29} steranes ($\mu\text{g/g}$); (f) $C_{19}\text{-}C_{23}\text{TT}/C_{30}\text{H}$ versus Triaromatic steranes ($\mu\text{g/g}$); (g) $C_{19}\text{-}C_{23}\text{TT}/C_{30}\text{H}$ versus Admantanes ($\mu\text{g/g}$); (h) $C_{19}\text{-}C_{23}\text{TT}/C_{30}\text{H}$ versus Diamondoids ($\mu\text{g/g}$).

Hydrocarbon mixing is indicated by the obvious discrepancy in evaluating thermal maturity of crude oils by using molecular biomarkers (Figure 10a) and diamondoids (Figure 10e), respectively. As stated below, for Group I oils, the mixing of crude oils generated from different sources with distinct thermal maturity levels is supposed to be

responsible partly for it. Moreover, Group I oils are extremely enriched in diamondoids and aromatic compounds (Figures 5 and 7). This may be caused by the high thermal maturity of their sources (Figure 10e), which facilitates the generation of these compounds resistant to thermal stress. On the other hand, multiple extensive gas charging and cap gas leakage from the reservoirs are also considered to play a part role as indicated by the loss of $n\text{-C}_{10}\text{--}n\text{-C}_{14}$ (Figure 12) [45], which agrees with previous studies [21,46]. For Group III/IV oils, this is assumed to be induced by the mixing of oils originated from the same source at different thermal maturity levels.

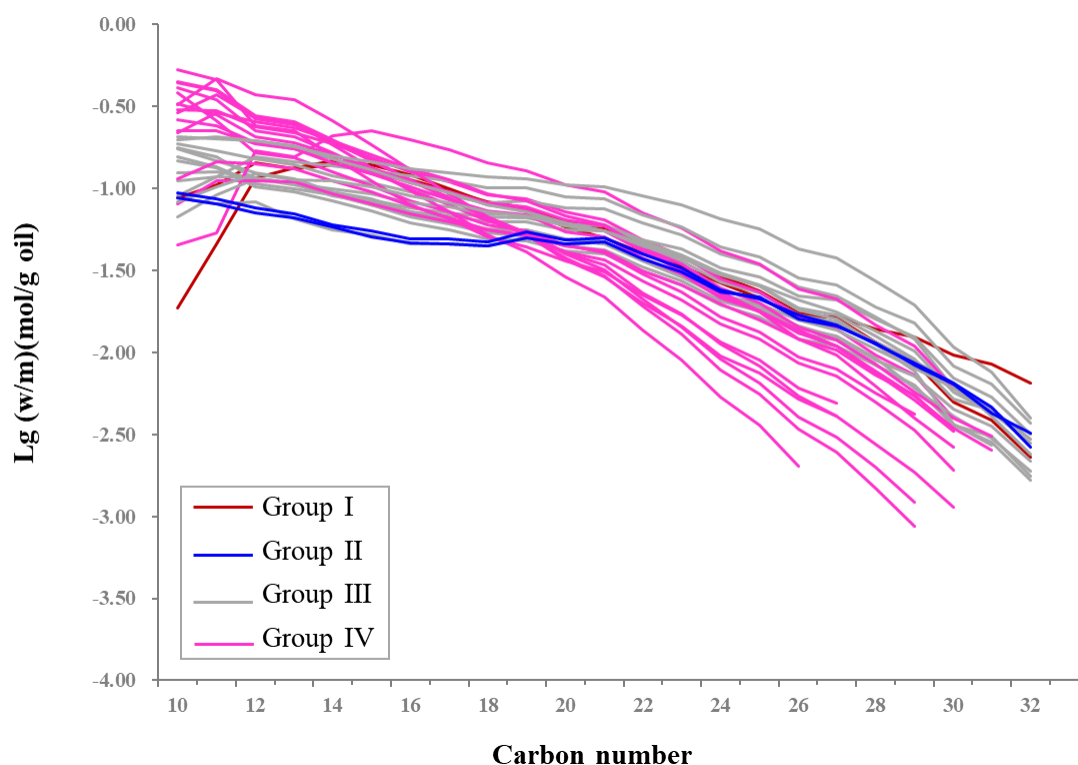


Figure 12. The crossplots of mole concentration versus carbon number of n -alkanes for collected oil samples, indicating the occurrence of gas washing in the Kekeya area.

4.3. Possible Oil Sources

In the Kekeya area, the Permian Pusige Formation and the Middle-Lower Jurassic Formations are considered to be the effective source rocks [5,8]. The two sets of source rocks show obvious differences in biomarkers, and the biomarkers within the Permian Pusige Formation are enriched in the unknown C_{30} terpenoids, C_{29} and C_{30} rearranged hopanes and C_{29} regular steranes [8,9]. While the Middle-Lower Jurassic source rocks contain less C_{30} rearranged hopanes and Ts, but more C_{29} regular steranes [9,11]. More importantly, the Permian source rocks and associated oils are isotopically lighter, the relevant Jurassic with the $\delta^{13}\text{C}$ values of individual n -alkanes range from -34.0% to -28.0% [9,10]. The $\delta^{13}\text{C}$ values of Jurassic kerogens extend from -27.2% to -23.3% [13], resulting in -30% to -26% for the $\delta^{13}\text{C}$ values of oils, since the thermal maturation effects usually induce $<3\%$ isotopic fractionation between parent kerogen and associated crude oil [47]. The relative enrichments of unknown C_{30} terpenoids, C_{29} and C_{30} rearranged hopanes (Figure 4c,d) and isotopically lighter n -alkanes (-32.4% to -27.6%) (Table 5) support that Group III/IV oils are derived mainly from the Permian Pusige Formation. Our current research demonstrates that the deep burial depth (8000–10,000 m) allows the Permian source rocks to approaching the high mature stage in the Kekeya structural belt ($\%Ro = 1.3\text{--}2.0$), shallow burial depth (4000–6000 m) leads to the formation of matured Permian source rocks in the Fusha structural belt ($\%Ro = 0.6\text{--}1.2$). Accordingly, the effective

Permian source rock for the high-matured Group III/IV oils should be located at the Kekeya structural belt.

Compared with Group III/IV oils, the relative depletion of C₃₀ rearranged hopanes and Ts and enrichment of C₂₉ regular steranes artificially indicate that the Jurassic source rocks may have the major contribution for Group II oils (Figure 3b). However, the isotopically light *n*-alkanes (−32.1% to −29.8%) suggests the Permian source rocks should play the major role (Figure 8). This discrepancy may be attributed to the lower thermal maturity levels of Group II oils. As stated above, Group II oils present lower thermal maturity than Group III/IV oils. This is indicated by the lower thermal maturity ratios including $\Sigma n\text{-C}_{21-} / \Sigma n\text{-C}_{22+}$, C₂₉ 20S/(20S + 20R), Ts/(Ts + Tm), C₁₉-C₂₃TT/C₃₀H, diaC₃₀H/C₃₀H, MDI and TA[C₂₀/(C₂₀ + C₂₈)-20R] (Tables 1–4), resulting in lower absolute concentrations of *n*-alkanes and diamondoids (Tables 2 and 3) and higher absolute concentrations of terpanes, steranes and triaromatic steranes within Group II oils (Tables 1 and 4) as well as 1–2% ¹³C-depleted *n*-alkanes (Figure 8). Group II oils were collected from the newly drilled discovery Well FS8 and are assumed to be derived from the local Permian source rocks that have the nearly same thermal maturity levels, since crude oil and the local Permian source rocks share have the nearly same thermal maturity levels. More importantly, the Permian Pusige Formation of Well FS4 has the similar burial depth and hence thermal maturity levels as Well FS8. While the produced oils from the Cretaceous reservoir present greater thermal maturity levels as those oils from the Kekeya structural belt (Figure 10). This indicates oil secondary migration from the Kekeya to Fusha structural belt around Well FS4 (Figure 3b–d).

In comparison with Group III/IV oils, Group I oils show a relative depletion of tricyclic terpanes (Ts), C₃₀ rearranged hopane, and an enrichment in C₂₉ Norhopane, C₃₀-C₃₅ hopanes, and C₂₉ steranes (refer to Table 1). The δ¹³C values of individual *n*-alkanes range from −30.2% to −26.1%, resulting in isotopically 2–3% heavier than that for Group III/IV oils. This is generally consistent with the molecular and isotopic compositions of oils generated from the Jurassic source rocks, indicating the contribution of Jurassic source rocks for Group I oils. It is only constrained around the location of Well KS101, since no vital geochemical diagnostic can be detected to indicate the relevant input of Jurassic-associated oils in the other wells. This may be attributed to the vertically permeable passageways around Well KS101, which is indicated by the strong gas washing and leakage (Figure 12) [21,46]. Moreover, its greater burial depth after subsidence from 65–20 Ma results in enough oil can be generated from Jurassic source rocks and then migrate upward to the Cretaceous reservoirs [4,19,48].

However, the Permian source rocks also play a part role. These two oils contain extremely high concentrations of diamondoids and aromatic compounds (Figures 5 and 7). The diamondoids indicate the thermal maturity levels of %Ro = 1.6–1.9 for Group I oils (Figure 10e), which is much greater than that of terpanes and steranes (%Ro = 0.6–0.8) (Figure 10a–d). This discrepancy indicates the mixing of Permian-sourced high-matured oils and Jurassic-sourced matured oils, because the local Jurassic source rocks are located mainly within the matured source kitchen and have not approached the high maturity level in study area [3,12,14]. Less input of isotopically heavier Jurassic-sourced oils lead to lighter δ¹³C values of individual *n*-alkanes for oil sample from the upper part of Cretaceous reservoirs of Well KS101 relative to the lower one.

In general, Group I oils are a mixture of the Jurassic-associated matured oil and Permian-sourced high-matured oil. Group II oils were generated from the matured Permian Pusige shale sequences in the Fusa structural belt without the contribution of secondary migrated oil from the Kekeya structural belt. Group III/IV oils were derived mainly from the high-matured Permian Pusige source rocks in the Kekeya structural belt. The distribution patterns of molecular and stable carbon isotopic compositions of collected oils (except for Group I oils) are regulated mainly by thermal stress in this region. The Permian Pusige Formation is therefore supposed to be the major effective source rock in study area. The Middle-Lower Jurassic formations only act as a part role in the area of Well

KS101. As stated above, this conclusion partly agrees with the second-to-fourth thoughts and disagrees with the first thought regarding oil sources in study area. Accordingly, this study provides a better understanding of hydrocarbon sources and associated processes of relevant petroleum systems, which should be useful in making a reasonable strategy for petroleum exploration in this region.

5. Conclusions

This study presents the comprehensive quantitative data of molecular and stable carbon isotopic compositions of crude oils from the Kekeya area of Southwest Depression, Tarim Basin, to clarify oil groups and effective oil sources. The following conclusions can be made:

- (1) Lacustrine shale sequences within the Upper-Middle Permian Pusige Formation (P_{3-2p}) are the major effective oil sources. In the Kekeya structural belt, crude oils were generated from deeply buried P_{3-2p} at the late-to-high maturity stage. In the Fusha structural belt, oils produced from the Lower-Jurassic reservoirs (J_{1s}) were generated from the local P_{3-2p} at the middle to late mature stage. The P_{3-2p} -associated oils in the Kekeya structural belt can migrate laterally to the Fusha structural belt, but not to the location of Well FS8;
- (2) The Middle-Lower Jurassic lacustrine shales (J_{1-2}) as the second effective sources are only confined to the area of Well KS101 in the Kekeya structural belt. The J_{1-2} generated oils can migrate upward and into the Cretaceous sandstone reservoirs of Well KS101, and then mingle with the early charged oils derived from the Permian source rocks;
- (3) The comprehensive quantitative data of crude oils can provide a better understanding of hydrocarbon groups, sources and accumulation process in the Kekeya area of the Southwest Depression, Tarim Basin. Our future work will combine the results of 1D and 2D basin modeling with geochemical data together to make a more sophisticated constrains. This should be useful for petroleum exploration in this region.

Author Contributions: X.G.: Investigation, Formal analysis, Data curation, Writing—original draft. Q.X.: Methodology, Conceptualization, Project administration, Data Curation, Writing—Review & Editing. Z.G.: Investigation, Formal analysis. S.C.: Investigation, Methodology. H.Z.: Validation, Funding acquisition. X.W.: Supervision, Funding acquisition, Resources. Z.X.: Supervision, Validation, Funding acquisition. Z.W.: Supervision, Validation, Funding acquisition, X.X.: Project administration, Supervision. Q.M.: Supervision, Project administration. All authors have read and agreed to the published version of the manuscript.

Funding: We appreciate the grants from National Nature Science Foundation of China (No. 42073066, 41961144023, 41673041), the State Key Laboratory of Organic Geochemistry, GIGCAS (No. SKLOG202013), and the Key Laboratory of Exploration Technologies for Oil and Gas Resources (Yangtze University), Ministry of Education (No. PI2021-05).

Data Availability Statement: Data are contained within the article.

Conflicts of Interest: Authors Haizhu Zhang, Xiang Wang, Zhenping Xu were employed by the company PetroChina Tarim Oilfield Branch. The remaining authors declare that the research was conducted in the absence of any commercial or financial relationships that could be construed as a potential conflict of interest. All authors have read and agreed to the published version of the manuscript.

References

1. Jia, C. *Tectonic Characteristics and Petroleum of Tarim Basin China*; Petroleum Industry Press: Beijing, China, 1997; pp. 205–389.
2. Chen, J.; Yin, J.; Zhang, Y. Formation conditions of Kekeya anticlinal oil and gas reservoir. *Xinjiang Pet. Geol.* **1996**, *17*, 219–224.
3. Yang, B.; Liu, Y. Source rock evaluation and exploration direction in southwest depression of Tarim Basin. *Xinjiang Pet. Geol.* **1992**, *13*, 339–350.
4. He, D.; Chen, H.; Liu, S.; Zhu, R.; Deng, X. Reservoir formation mechanism of Kekeya condensate oil and gas field. *Pet. Explor. Dev.* **1997**, *24*, 28–32.

5. Huang, W.; Pan, C.; Yu, S.; Zhang, H.; Xiao, Z.; Zhang, Z. Source and filling process of crude oil from Fusha 4 well in the Kedong structural belt of the southwestern Tarim depression. *Nat. Gas Geosci.* **2022**, *32*, 1836–1847.
6. Mo, W.; Lin, T.; Zhang, Y.; Yi, S.; Wang, D.; Zhang, L. Oil and gas sources and reservoir formation models of the Kedong Kekeya structural belt in the front of the West Kunlun Mountains. *Pet. Exp. Geol.* **2013**, *35*, 364–371.
7. Wang, J.; Gao, Z.; Kang, Z.; Yang, Y.; Wei, D.; Qin, N. Sedimentary environment and organic geochemical characteristics of hydrocarbon source rocks of Pusige Formation in Hetian Sag, Southwest Tarim Depression, Tarim Basin. *Nat. Gas Geosci.* **2017**, *28*, 1723–1734.
8. Tang, Y.; Hou, D.; Xiao, Z. Geochemical Characteristics and Oil Source of Crude Oil in the Kekeya Oilfield. *Miner. Rock Geochem. Bull.* **2006**, *25*, 160–162.
9. Du, Z.; Zeng, C.; Qiu, H.; Yang, Y.; Zhang, L. Characteristics of two sets of Permian source rocks and oil source analysis of Kedong 1 well in Yecheng Depression, southwestern Tarim Basin. *J. Jilin Univ. Earth Sci. Ed.* **2016**, *46*, 651–660.
10. Wang, Q.; Peng, P.; Zeng, J.; Zou, Y.; Yu, C.; Zhang, B.; Xiao, Z. Oil source analysis of condensate oil and Kekeya crude oil from Kedong 1 well in Yecheng Depression. *Geochemistry* **2014**, *43*, 469–476.
11. Xiao, Z.; Tang, Y.; Hou, Y.; Zhang, Q.; Wang, F.; Lu, Y. Oil source study of Kekeya condensate reservoir. *J. Sedimentol.* **2002**, *20*, 716–720.
12. Li, S.; Kang, Z.; Qiu, H.; Meng, M.; Feng, Z.; Li, S. Hydrocarbon accumulation model in southwest depression of Tarim Basin. *Geol. China* **2014**, *41*, 387–398.
13. Ding, Y.; Qiu, F.; Li, G. Comparative analysis of oil and gas sources in southwest depression of Tarim Basin. *Xinjiang Geol.* **2000**, *18*, 61–67.
14. Lv, M. A preliminary study on oil source in the western Tarim Basin. *J. Pet.* **1981**, *3*, 31–36.
15. Wang, Y.; Yang, B. Discussion on oil source of southwest depression in Tarim Basin. *Xinjiang Pet. Geol.* **1987**, *4*, 33–39.
16. Dai, Q.; Mei, B. Diagenetic products of resin diterpenes and their thermal transformation. *Oil Gas Geol.* **1988**, *2*, 115–124.
17. Gong, D.; Wang, Z.; Liu, G.; Chen, G.; Fang, C.; Xiao, Z. Re-examination of the oil and gas origins in the Kekeya gas condensate field, northwest China—a case study of hydrocarbon-source correlation using sophisticated geochemical methods. *Acta Geol. Sin.* **2017**, *91*, 186–203. [[CrossRef](#)]
18. Hu, J.; Wang, T.; Chen, J.; Cui, J.; Zhang, B.; Shi, S.; Wang, X. Geochemical characteristics and genesis types of crude oil in the periphery of the Taxinan depression. *J. Pet.* **2015**, *36*, 1221–1233.
19. Li, M.; Lin, R.; Liao, Y.; Snowdon, L.R.; Wang, P.; Li, P. Organic geochemistry of oils and condensates in the Kekeya Field, Southwest Depression of the Tarim Basin (China). *Org. Geochem.* **1999**, *30*, 15–37. [[CrossRef](#)]
20. Wang, Q.; Yang, H.; Li, Y.; Cai, Z.; Yang, X.; Xu, Z.; Chen, C.; Sun, C. Major breakthrough and exploration prospect of Carboniferous - Permian system in Well Qiatan 1, southwest mountain front area. *China Pet. Explor.* **2023**, *28*, 34–45.
21. Huang, W.; Yu, S.; Zhang, H.; Xiao, Z.; Liu, D.; Pan, C. Diamondoid fractionation and implications for the Kekeya condensate field in the southwestern depression of the Tarim basin, NW China. *Mar. Pet. Geol.* **2022**, *138*, 0264–8172. [[CrossRef](#)]
22. Xiao, Q.; Sun, Y.; Zhang, Y.; Chai, P. Stable carbon isotope fractionation of individual light hydrocarbons in the C6–C8 range in crude oil as induced by natural evaporation: Experimental results and geological implications. *Org. Geochem.* **2012**, *50*, 44–56. [[CrossRef](#)]
23. Xiao, Q.; Cai, S.; Liu, J. Microbial and thermogenic hydrogen sulfide in the Qianjiang Depression of Jiangnan Basin: Insights from sulfur isotope and volatile organic sulfur compounds measurements. *Appl. Geochem.* **2021**, *126*, 104865. [[CrossRef](#)]
24. Peters, K.E.; Walters, C.C.; Moldowan, J.M. Origin and preservation of organic matter. In *The Biomarker Guide*; Cambridge University Press: Cambridge, UK, 2004.
25. Connan, J.; Cassou, A.M. Properties of gases and petroleum liquids derived from terrestrial kerogen at various maturation levels. *Geochim. Cosmochim. Acta* **1980**, *44*, 1–23. [[CrossRef](#)]
26. Sofer, Z. Stable carbon isotope compositions of crude oils: Application to source depositional environments and petroleum alteration. *Am. Assoc. Pet. Geol. Bull.* **1984**, *68*, 31–49.
27. Shanmugam, G. Significance of coniferous rain forests and related organic matter in generating commercial quantities of oil, Gippsland Basin, Australia. *Am. Assoc. Pet. Geol. Bull.* **1985**, *69*, 1241–1254. [[CrossRef](#)]
28. Hughes, W.B.; Holba, A.G.; Dzou, L.I.P. The ratios of dibenzothiophene to phenanthrene and pristane to phytane as indicators of depositional environment and lithology of petroleum source rocks. *Geochim. Cosmochim. Acta* **1995**, *59*, 3581–3598. [[CrossRef](#)]
29. Zeng, C.; Zhang, L.; Lei, G.; Chen, Y.; Zhang, X. Comparison of source rock biomarker characteristics and sedimentary environment indication significance in the southwestern Tarim Depression. *Xinjiang Geol.* **2011**, *3*, 319–323.
30. Zhuang, X.; Xiao, L.; Yang, J. Distribution and evolution of sedimentary facies in southwest Tarim Basin. *Geol. Xinjiang* **2002**, *51*, 78–82.
31. Xia, H.; Liu, Z.; Yuan, W. Jurassic sedimentary basin and sedimentary facies in the Zimgen-Sangzhuhe area. *Xinjiang Geol.* **2002**, *20*, 67–71.
32. Zumber, J.E. Prediction of source rock characteristics based on terpane biomarkers in crude oils: A multivariate statistical approach. *Geochim. Cosmochim. Acta* **1984**, *51*, 1625–1637. [[CrossRef](#)]
33. Smith, A.B.; Littlewood, D.T. Paleontological data and molecular phylogenetic analysis. *Paleobiology* **1994**, *20*, 259–273. [[CrossRef](#)]
34. Philp, R.P.; Gilbert, T.D. Biomarker distributions in Australian oils predominantly derived from terrigenous source material. *Org. Geochem.* **1986**, *10*, 73–84. [[CrossRef](#)]

35. Grice, K.; Audino, M.; Boreham, C.J.; Alexander, R.; Kagi, R.I. Distributions and stable carbon isotopic compositions of biomarkers in torbanites from different palaeogeographical locations. *Org. Geochem.* **2001**, *32*, 1195–1210. [[CrossRef](#)]
36. Grantham, P.J.; Wakefield, L.L. Variations in the sterane carbon number distributions of marine source rock derived crude oils through geological time. *Org. Geochem.* **1988**, *12*, 61–73. [[CrossRef](#)]
37. Kodner, R.B.; Pearson, A.; Summons, R.E.; Knoll, A.H. Sterols in red and green algae: Quantification, phylogeny, and relevance for the interpretation of geologic steranes. *Geobiology* **2008**, *6*, 411–420. [[CrossRef](#)] [[PubMed](#)]
38. Huang, W.; Meinschein, W.G. Sterols as ecological indicators. *Geochim. Cosmochim. Acta* **1979**, *43*, 739–745. [[CrossRef](#)]
39. Douaa, F.; Arafa, F.E.; Walid, A.M.; Atef, M.H. Organic geochemical signals of Paleozoic rocks in the southern Tethys, Siwa basin, Egypt: Implications for source rock characterization and petroleum system. *Phys. Chem. Earth Parts A/B/C* **2023**, *130*, 103393.
40. Seifert, W.K.; Moldowan, J.M. Use of biological markers in petroleum exploration. *Methods Geochem. Geophys.* **1986**, *24*, 261–290.
41. Dzou, L.I.P.; Noble, R.A.; Senftle, J.T. Maturation effects on absolute biomarker concentration in a suite of coals and associated vitrinite concentrates. *Org. Geochem.* **1995**, *23*, 681–697. [[CrossRef](#)]
42. Aqino Neto, F.R.; Trendel, J.M.; Restle, A.; Connan, J.; Albrecht, P.A. Occurrence and formation of tricyclic and tetracyclic terpanes in sediments and petroleum. In *Advances in Organic Geochemistry 1981: International Conference Proceedings, Bergen, Norway, 14–18 September 1981*; Bjory, M., Ed.; John Wiley & Sons Ltd.: New York, NY, USA, 1983; pp. 659–667.
43. Peters, K.E.; Moldowan, J.M.; Sundararaman, P. Effects of hydrous pyrolysis on biomarker thermal maturity parameters: Monterey Phosphatic and Siliceous members. *Org. Geochem.* **1990**, *15*, 249–265. [[CrossRef](#)]
44. Chen, J.; Fu, J.; Sheng, G.; Liu, D.; Zhang, J. Diamondoid hydrocarbon ratios: Novel maturity indices for highly mature crude oils. *Org. Geochem.* **1996**, *25*, 179–190. [[CrossRef](#)]
45. Kissin, Y. Catagenesis and composition of petroleum: Origin of n-alkanes and isoalkanes in petroleum crudes. *Geochim. Cosmochim. Acta* **1987**, *51*, 2445–2457. [[CrossRef](#)]
46. Zhang, M.; Huang, G.; Zhao, H.; Wang, X. Genetic characteristics of condensate reservoirs in Kekeya area, Tarim Basin. *Chin. Sci. Earth Sci.* **2008**, *38*, 17–23.
47. Lewan, M.D. Effects of thermal maturation on stable organic carbon isotopes as determined by hydrous pyrolysis of woodford shale. *Geochim. Cosmochim. Acta* **1983**, *47*, 1471–1479. [[CrossRef](#)]
48. Xiao, A. Formation and hydrocarbon accumulation of Kekeya Structure in Southwest Depression of Tarim Basin. In *Proceedings of the International Seminar on Hydrocarbon Accumulation Mechanism and Hydrocarbon Resource Evaluation, Beijing, China, 1996*; Editorial Board of Oil and Gas Accumulation Research Series, Ed.; pp. 116–120+325.

Disclaimer/Publisher’s Note: The statements, opinions and data contained in all publications are solely those of the individual author(s) and contributor(s) and not of MDPI and/or the editor(s). MDPI and/or the editor(s) disclaim responsibility for any injury to people or property resulting from any ideas, methods, instructions or products referred to in the content.